19

Energy Limits for Life in the Subsurface

DOUG LAROWE AND JAN AMEND

19.1 Introduction

Life's demand for energy drives rapid exchanges of carbon between the atmosphere, oceans, and land (1). Photosynthesis and respiration of organic carbon on and near the surface of Earth account for the vast bulk of the transfers of carbon between these reservoirs, processes that dwarf geologic sources and sinks of carbon on short timescales (2; Chapter 16, this volume). In recent years, however, it has become apparent that Earth hosts a vast subsurface biosphere (3–16) that operates much more slowly (17–20) than surface life. It is not clear to what depth this biosphere exists, the rates at which it is active, what reactions are being catalyzed for energy, or what impact it has had on Earth's carbon cycle through time. Extrapolating metabolic rates on Earth's surface to the subsurface is complicated by an essential difference – the types and rates of biological activity on the surface are determined by daily and seasonal cycles driven by the sun, but life in the subsurface seems to be more attuned to geologic processes and timescales. Such slow rates make it difficult to study subsurface life, but the biological demand for energy can be used to better understand the rates at which these organisms are active and how they interact with their geochemical environments. Studying subsurface life can therefore help reveal the energy limits for life and thus its spatial and temporal extent.

In addition to hosting organisms on the low end of the bioenergetic spectrum, the potential size of the subsurface biosphere motivates many researchers studying deep life. Marine sediments alone have been estimated to contain 10^{29}–10^{30} microbial cells (4, 5) and occupy 300 million km^3, over 22% of the volume of Earth's oceans (21). A similar number of microorganisms are thought to inhabit the continental subsurface (9, 22; Chapter 17, this volume). Cells have been found as deep as 3.5 km beneath the surface of land, which, if true of all continental crust, would translate to a potential habitable volume of over 730 million km^3 (taking the total continental crust surface to be 2.1×10^8 km^2; 23). Although there are no estimates of the size of the ocean crustal basement biosphere, if the top 600 m of it is sufficiently hydrologically permeable to host life (24–32), this would correspond to 1.8 billion km^3 (based on the ocean crust covering 68.8% (2.99×10^8 km^2) of Earth's surface; 23). Most recently, it has been estimated that the deep subsurface contains about 13% of the biomass on the planet (10).

Finally, although we have no information about current or past life on extraterrestrial bodies in our solar system, it is most likely that any evidence of it will be in the subsurface (33–35).

Cell counts, microbial cultivation work, and molecular biological efforts are helping to describe the numbers, viability, activity levels, and variety of microorganisms in subsurface environments (Chapters 17 and 18, this volume). However, the relative inaccessibility of these environments, the difficulty of cultivating representative microorganisms, and the long timescales associated with some of their lifestyles are major impediments to obtaining a comprehensive understanding of complex subsurface ecosystems. Hence, modeling approaches that include geochemical data as well as typical microbiological measurements can be useful strategies for quantifying biogeochemical interactions in the subsurface. Because all living things must catalyze redox reactions to obtain energy and the amount of energy available from a chemical reaction depends strictly on the prevailing environmental conditions, energy-based modeling provides a framework for quantifying microbial processes in any setting. In this chapter, we will discuss what is known about the microbial demand for energy in low-energy settings, review recent efforts to quantify the energy available in subsurface habitats, and provide an overview of how these calculations are carried out.

19.2 Microbial States

The physiological state of a microorganism is related to the rate at which it is using energy. In contrast to the four classical physiological states that microbial isolates exhibit in high-energy, high-nutrient, short-timespan laboratory experiments – lag, exponential, stationary, and death phases – microorganisms in nature are often nutrient and energy limited and exist in complex communities that are exposed to varying physiochemical properties such as oscillating temperature, pH, and water activity. Their physiological states do not necessarily correspond to those that have been determined in the laboratory and are in many instances unknown (20, 36). Consequently, the rate at which these organisms are processing carbon and energy in nature is not well constrained. Back of the envelope-style calculations reveal how unlikely widespread microbial growth is in nature: if every microorganism in the subsurface (~10^{30} organisms with ~10 fg C $cell^{-1}$) doubled every day, all of the carbon in Earth's crust (60 million Gt; 37) would become microbial biomass in less than 23 days.

Whatever the physiological status of living microorganisms in natural settings, their use of energy can be partitioned into two broad categories: maintenance and growth. It is difficult to strictly separate maintenance and growth activities because when organisms are growing, they are also carrying out maintenance functions. Similarly, the critical maintenance activity of replacing biomolecules is an aspect of the anabolic processes that lead to growth. Nonetheless, they are commonly viewed as distinct states with particular energetic ramifications.

Maintenance generally refers to the collections of activities that an organism performs to simply stay alive. It can include nutrient uptake, motility, the preservation of charged

membranes, excretion of (bio)molecules, and changes in stored nutrient concentrations (see 38 for a review). It is difficult to determine the amounts of energy that each of these and other maintenance functions require, so they are typically lumped together and defined in the negative: all of the activities that a microorganism carries out that are not associated with growth. Traditionally, maintenance energies are determined by *growing* microorganisms at ever-slower rates and extrapolating the amount of energy that they use to a value that would represent zero growth (for a review, see 17). Values reported in the literature range over more than five orders of magnitude, from 0.019 fW (fW ≡ femtowatts, 10^{-15} J s^{-1}) for anoxygenic phototrophy to 4700 fW for aerobic heterotrophy (see 39). This procedure might decipher the energy partitioned into nongrowth activities for a high-energy state – *growth* – but maintenance energies in nature are orders of magnitude lower than these values (17, 18, 39–41).

To distinguish laboratory measurements of maintenance from the survival state of microorganisms in nongrowing and other low-energy environments, the term "basal power requirement" has been introduced (17). The use of the word "power" instead of "energy" is apt (see 39, 41, 42) since so-called maintenance energies are given in units of energy per time. Recent results from modeling studies support the notion that in very-low-energy settings (e.g. deep oligotrophic marine sediments such as those under the South Pacific Gyre), maintenance powers are indeed several orders of magnitude lower than those reported in the literature, from 50 to 3500 zW $cell^{-1}$ (where zW ≡ zeptowatt, 10^{-21} W; 41). Related calculations suggest that the amount of particulate organic matter required to sustain microbes at a basal power level in the same oligotrophic environment is equivalent to about 2% of their biomass carbon per year (36). It should be noted that these latter two studies assume that all of the energy used by these microbes is for maintenance only, not growth. It is not known whether microorganisms in ultra-low-power settings produce daughter cells or merely persist via maintenance (17, 18, 20). It is thought that very slow or no growth is the norm in many environments (43), especially chemically stagnant, low-energy ones such as oligotrophic marine sediments (17, 44–46). However, it should be noted that when conditions improve, metabolic rates can increase dramatically (47). Although values are not well constrained for dynamic ecosystems, maintenance power can vary due to many factors, including temperature (for the same species), substrate identity, redox conditions, and cultivation techniques (18).

Microbial growth can refer to the generation of new cells, the production of biomass accompanying enlarging cells and the synthesis of external structures such as stalks, sheaths, tubes, biofilms, and other polymeric saccharides. Although extracellular biomass can be a significant fraction of the total biomass of a system, most efforts to quantify the amount of energy that it takes to make biomass have focused on the energetics of making cells, and like all chemical reactions, the amount of energy required to synthesize cells depends in large part upon the physiochemical properties of the environment. The first modern effort to explicitly quantify how environmental parameters influence the energetics of biomass synthesis focused on how the redox state of the environment influences the energy required to synthesize the biomolecules that make up cells (48). More recently,

LaRowe and Amend (49) expanded this analysis to quantify the amount of energy required to make biomass as a function of temperature, pressure, redox state, the sources of C, N, and S, and cell mass, while also accounting for the polymerization of monomers into biomacromolecules such as proteins, DNA, RNA, and polysaccharides (see below). These kinds of modeling results depend on both the compositions and the masses of microbial cells. The stoichiometry of biomass varies considerably (see 18, 49 for reviews), with the average nominal oxidation state of carbon (NOSC; see 50) in cell biomass – a tidy numerical representation of the ratio of carbon to hydrogen, nitrogen, oxygen, sulfur, and phosphorous in organic matter – varying from at least from +0.89 to –0.45 (49). Note that the commonly used stand-in for biomass, "CH_2O," fixes the NOSC at 0. As with maintenance power, cell stoichiometry varies with environmental conditions (see 49).

Other attempts to account for the energy required to make biomass rely upon laboratory experiments that are designed to promote growth, conditions that are rarely encountered in the subsurface (see 39 for a review). In addition, numerous energy-based models developed to predict biomass yields have limited applicability because they are restricted to standard and/or reference states (for reviews, see 39, 51). Most of these models fix biomass yield coefficients, which leads to predictions of equal biomass production (for the same synthesis reactions) under potentially very different environmental conditions. Other efforts seeking to determine the amount of energy required to make biomass rely on estimates of the number of moles of ATP that are required to carry out various aspects of biomolecular synthesis. A commonly cited version of this approach (52) reports the ATP requirements for various anabolic and maintenance functions. The reference for these values ultimately cites a paper (53) that effectively assumes the amount of ATP required for a variety of biochemical processes with little to no experimental evidence or references. Even if the amount of ATP required to synthesize biomass were well constrained in natural settings, the amount of energy that is released from the hydrolysis of ATP to ADP and phosphate is a function of the physiochemical characteristics of the environment in which it is happening, and therefore not a constant (54–56).

Microorganisms can also enter into low-energy and dormant states. While some authors use the term "dormancy" to describe low-energy states as well (57), others reserve this term for true endospore-forming microorganisms that are metabolically inactive (58). *Sensu stricto*, dormancy is a reversible, contingent state that is entered into when resources become limiting. Because there is no metabolic activity, critical functions such as DNA and protein repair are not possible. As a result of abiotic hydrolysis, oxidation, and other degradative processes, dormant organisms have a finite lifespan. Although little is known about the energetics or maximum possible length of dormancy (18, 43), there is evidence that revival rates are inversely correlated with the amount of time a microorganism spends in the dormant state (43, 59), an observation that has been included in modeling studies of microbial dormancy (60, 61). One study showed that the number of endospores in frozen samples decreases with sample age since endospores do not have active DNA-repair mechanisms, but that low-energy bacteria in the same samples can survive for up to half a million years (62).

Microorganisms in low-energy states, in contrast to dormant ones, are able to slowly metabolize in order to remain viable for potentially millions of years (19, 40). These low-energy states are thought to be prevalent in natural systems, to exist on a spectrum of levels, and to have multiple entry points (57). In fact, it is possible that $<10\%$ of microbial cells in soil and aquatic environments are active (63). One estimate proclaimed that low-energy cells can exist on three orders of magnitude lower power than typical maintenance power levels (64), though, as pointed out above, maintenance powers determined under relatively high-energy conditions span five orders of magnitude. Perhaps energy usage in the low-energy state is more akin to basal maintenance power as defined by Hoehler and Jørgensen (17): the flux of energy required for a minimum survival state. Some speculate that virtually all microbial cells in deep marine sediments are surviving in ultra-low energy states (20). A recent modeling study represented the cells in an oligotrophic marine sediment section as existing in a series of ever-lower energy states, but none as truly dormant (36).

19.3 Gibbs Energy: Where It Comes from and How to Use It

All organisms catalyze reactions as they acquire energy from the environment and carry out biochemical functions related to maintenance and growth. The amount of energy associated with these chemical transformations depends on the exact identity of the reaction – all of the reactants and products describing the mass- and charge-balanced process – as well as the prevailing temperature, pressure, and composition of the environment in which it is happening. The mathematical approach that is used to quantify the change in energy resulting from a chemical reaction is the Gibbs function, denoted by G. Despite being well known, it is worth noting why this, of several energy functions related to the internal energy of a system, is the one that is used to assess how energy is required by organisms to perform a given task and how much energy results from catalyzing reactions that ultimately fuel life's demands. For textbook-level overviews of thermodynamics, see (65–68).

Because there is no absolute energy scale, we can only discuss changes in the amount of energy that a system contains. The change in the internal energy (U) of a system can be quantified by assessing changes in the temperature (T), pressure (P), volume (V), and entropy (S) of it, quantities that can be modified by the exchange of heat and matter between the system and the surroundings as well as reactions happening within the system. Changes in the internal energy of the system, dU, can be mathematically linked to how these four variables change in different ways (i.e. the various energy functions are effectively different partial derivatives of U with respect to T, P, V, and S). These four variables are known as state variable because they describe the state of the system at any given moment; functions including these variables are known as state functions. For instance, the change in the amount of heat (or enthalpy, H) associated with a system at constant pressure, dH_P, with no chemical reactions occurring, can be defined

by $dH_P = dU + PdV$, which is a simple statement of the first law of thermodynamics – the conservation of energy (technically, this and other state functions hold for infinitesimal changes taking place in the time interval t to $t + dt$). Enthalpy is a useful state function that describes the evolution of the heat content of a system, but it cannot predict how the system will evolve. The Gibbs energy function accomplishes this by combining the first law of thermodynamics with the second law, which essentially states that the entropy of an isolated system cannot decrease (see Box 19.1).

Box 19.1 Entropy, affinity, and the reaction progress variable.

Entropy is sometimes wrongly discussed in terms of being equivalent to "disorder." This confusion likely arises from Boltzmann's statistical mechanical interpretation of entropy being related to the number of microstates that a system can occupy – the more microstates, the higher the entropy. The proliferation of the use of the word "entropy" in other fields (e.g. Shannon entropy in information theory, which is more akin to uncertainty than the classical definition of entropy as a quantity of energy) has contributed to the popular conception of entropy as a measure of disorder. From its origins with Carnot and developments by Clausius, de Donder, and Kelvin, entropy is described as a quantity of energy and a state variable; its units are J K^{-1} mol^{-1}. The classical definition of entropy is that it is equal to the change in the heat of a system, Q, at a given temperature: $dS = dQ/T$.

Prigogine and Defay (69) describe two ways in which the entropy of a system can change: (1) entropy can be transported across the boundary of a system and therefore be positive or negative; and (2) entropy can be generated inside of an isolated system due to the occurrence of chemical reactions – these reactions are irreversible and the net change of entropy associated with them is always positive, $dS > 0$. It is this inequality that ultimately specifies the direction in which a system will evolve. So, we can say that the entropy of a system changes due to entropy exchanges with the surroundings (dS_e) and entropy created within the system, dS_i, or $dS = dS_e + dS_i$. Because dS_i is related to the degree to which chemical reactions are occurring, it is in turn related to the extent to which a reaction has occurred. The extent of a reaction is known as ξ, and sometimes is called the reaction progress variable (69–71). Changes in the reaction progress variable for a reaction are related to the stoichiometric coefficients of the ith species in that reaction, v_i, by

$$\frac{dn_i}{v_i} = d\xi, \tag{19.a}$$

where n_i refers to the number of moles of the ith species produced or consumed in the reaction. For example, the extent to which the reaction describing hydrogen-consuming sulfate reduction,

$$SO_4^{2-} + 4H_2 + H^+ \rightarrow HS^- + 4H_2O, \tag{19.b}$$

has progressed, $d\xi_{(19.b)}$, is given by

$$\frac{dn_{SO_4^{2-}}}{-1} = \frac{dn_{H_2}}{-4} = \frac{dn_{H^+}}{-1} = \frac{dn_{HS^-}}{1} = \frac{dn_{H_2O}}{4} = d\xi_{(19.b)}. \tag{19.c}$$

Clearly, when $dn_i = v_i$, $d\xi_{(19.b)} = 1$ and the reaction is said to have turned over.

The reaction progress variable and entropy are connected through what is known as chemical affinity, A, a term that is sometimes used to quantify how far a system is from equilibrium: $dS_i = Ad\xi \geq 0$ (this equation is also known as de Donder's fundamental inequality and can be thought of as another statement of the second law of thermodynamics). Although chemical affinity and the Gibbs energy of a reaction are related simply by $A = -\Delta G_r$, the two quantities have important conceptual differences. A is defined as the change in Gibbs energy resulting from changes in the reaction progress variable while pressure, temperature, and composition (n_k) are held constant (70, 71):

$$A = -\left(\frac{\partial G}{\partial \xi}\right)_{T,P,n_k}. \qquad (19.d)$$

As such, affinity relates irreversible chemical reactions to entropy production, while the Gibbs energy of a reaction is traditionally used in reference to equilibrium states and reversible processes (see 66). Furthermore, chemical affinity can be connected to reaction rate as a measure of the distance that reaction is from equilibrium (69, 70, 72, 73).

Within this conceptualization, thermodynamic rate-limiting terms have been developed in kinetic models that relate the rates of biologically catalyzed reactions to their distance from equilibrium, with reactions closer to equilibrium being slower than those further away (74–78). Finally, affinity and the rate of entropy production have in turn been used to develop more recent developments in the field of nonequilibrium thermodynamics, especially systems far from equilibrium and the establishment of dissipative structures, such as life (see 65).

Changes in the Gibbs energy at constant temperature and pressure are commonly expressed as $dG_{T,P} = dH - TdS$, or in integrated form, $\Delta G = \Delta H - T\Delta S$, but is more clearly linked to changes in the internal energy state of a system by $dG_{P,T} = dU + PdV - TdS$. By incorporating the second law of thermodynamics, the Gibbs energy function quantifies the tendency of a chemical reaction to proceed in a particular direction. That is, for a given chemical reaction, negative values of ΔG indicate that if a reaction occurs, the net result is the formation of products at the expense of reactants; the opposite direction occurs for positive values of ΔG. When $\Delta G = 0$, there is no net reaction and equilibrium has been reached.

Thus far, we have represented thermodynamics functions with simple letters like G and H. However, if we want to use these functions to calculate the energetics of real processes under specific environmental conditions, we must become familiar with the alphabet soup of subscripts and superscripts that modify and specify the meanings of terms such as G and H. As noted above, since we can only know how the energy of a system changes, the upper case Greek letter delta, Δ, is often placed in front of energy functions to signify changes in values of that function (e.g. ΔG and ΔH). These should be thought of in terms of the difference in, for example, the Gibbs energy of the system at one configuration versus another: $\Delta G = G_2 - G_1$. How the system evolved from state 1 to state 2 is irrelevant. When the subscript r is added, ΔG_r, for example, stands for the Gibbs energy of a reaction. These subscripts are straightforward accoutrements decorating thermodynamics functions, but the superscripts

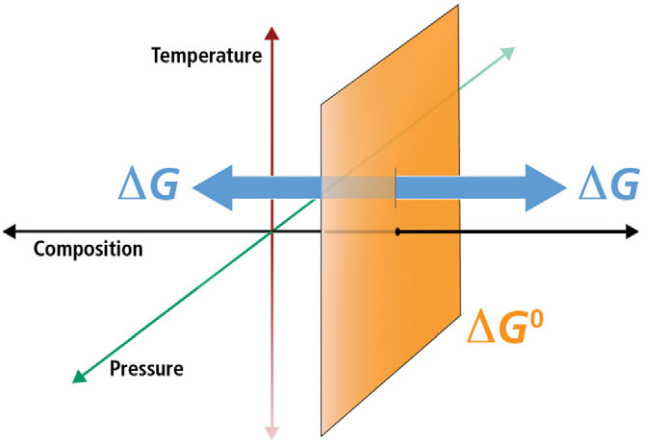

Figure 19.1 Schematic diagram illustrating the difference between standard-state Gibbs energies (ΔG_r^0) and overall Gibbs energies (ΔG_r) in temperature, pressure, and compositional space. For a given standard state, values of ΔG_r^0 refer to a fixed composition at any combination of temperatures and pressures (the orange plane) and that departures from this composition are what distinguish ΔG_r. For gases, pressure is part of the standard-state definition since the state of aggregation of a gas is partially determined by its partial pressure.

are less so, and they are typically more meaningful. When the superscript 0 appears, (i.e. ΔG^0), the symbol is explicitly referring to the change in Gibbs energy at a standard state. Standard states are one of the most frequently misunderstood aspects of thermodynamics.

The standard state used in traditional chemical thermodynamics does not refer to a temperature or pressure (i.e. it does *not* refer to 25°C and 1 bar), but a standard state of aggregation, or composition (see Figure 19.1 for a conceptual overview). The reason for this is that, as discussed above, we cannot know the internal energy, U, of a system, but we can determine changes in it. Both Gibbs energies and enthalpies are partial derivatives of U, so to quantify ΔG^0, ΔH^0, and other such standard state terms, we need a coherent system that relates the thermodynamic functions describing compounds to a set of standards. The system that is used in chemical thermodynamics to define the Gibbs energies and enthalpies of chemical compounds is related to that of the elements. For example, the standard-state Gibbs energy of formation from the elements of gaseous methane, $\Delta G^0_{CH_4(g)}$, is calculated based on the change of Gibbs energy associated with the reaction:

$$C_{\text{graphite}} + 2H_{2(g)} = CH_{4\ (g)}, \tag{19.1}$$

or:

$$\Delta G_r^0 = \Delta G^0_{CH_4(g)} - \Delta G^0_{C,graphite} - 2\Delta G^0_{H_2(g)}, \tag{19.2}$$

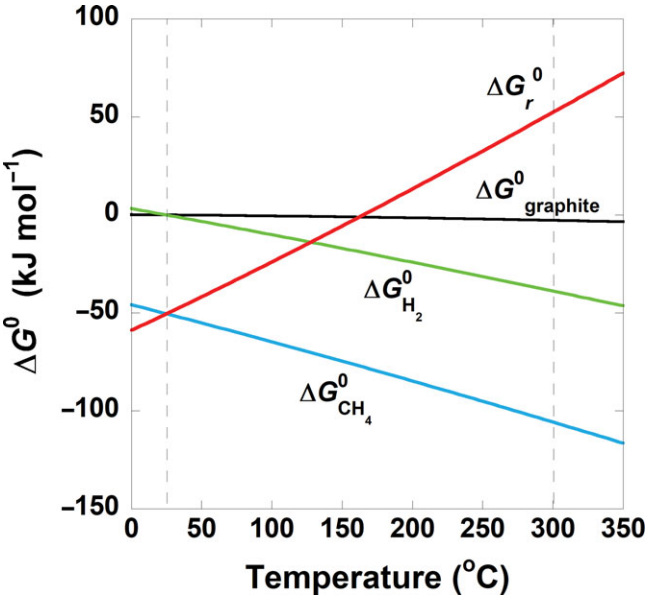

Figure 19.2 Standard-state Gibbs energies (ΔG^0) of H_2 gas, carbon as graphite, CH_4 gas, and the reaction defining the formation of methane from the elements as a function of temperature (see (19.1) and (19.2)). The vertical dashed lines at 25°C and 300°C are marked in reference to the examples discussed in the text.

where $\Delta G^0_{C,\,graphite}$ and $\Delta G^0_{H_2(g)}$ refer to the standard-state Gibbs energies of formation for elemental carbon as graphite and gaseous dihydrogen, respectively, and ΔG^0_r denotes the standard-state Gibbs energy of (19.1). These compounds are chosen because they are the stable phases of these two elements at the reference conditions of 25°C and 1 bar. The phase and form of the standard-state Gibbs energies and enthalpies of most elements are defined as those that are stable at 25°C and 1 bar, and they are all taken to be zero only at this temperature and pressure – their values are *not* zero at other combinations of temperature and pressure.

Staying with the CH_4 example, since the values of $\Delta G^0_{C,\,graphite}$ and $\Delta G^0_{H_2(g)}$ are 0 J mol^{-1} at 25°C and 1 bar and the value of ΔG^0_r for (19.1) is –50.4 kJ mol^{-1}, then $\Delta G^0_{CH_4(g)}$ = –50.4 kJ mol^{-1} at 25°C and 1 bar (the value of ΔG^0_r is determined from a series of calorimetric measurements that are beyond the scope of this chapter). At any other combination of temperature and pressure, values of $\Delta G^0_{C,\,graphite}$ and $\Delta G^0_{H_2(g)}$ are not 0 J mol^{-1} and therefore the value of ΔG^0_r does not equal that of $\Delta G^0_{CH_4(g)}$ (see Figure 19.2). For instance, at 300°C and 86 bars, they are –2.8 and –38.8 kJ mol^{-1}, respectively, and ΔG^0_r for (19.1) is –25.24 J mol^{-1}. Therefore, $\Delta G^0_{CH_4(g)}$ = –105.6 kJ

mol^{-1} at 300°C and 86 bars, more than twice the value at 25°C and 1 bar. Beyond stipulating that the forms of the elements that are used in calculating the Gibbs energies of formation are their stable ones at 25°C and 1 bar, temperature and pressure are not part of the definition of standard-state properties for substances, except for the standard state for gases (see below). Although this is a rather tedious discussion, it is presented to illustrate how temperature and pressure are properly taken into account in thermodynamic calculations, which are particularly important for quantifying the energetics of biogeochemical processes in the subsurface.

In addition to specifying that the definition of the chemical standard state relates thermodynamic properties of chemical species to those of the elements at particular combinations of temperature and pressure, it also specifies the state of aggregation of chemical substances. The commonly used standard state of aggregation differs depending on the phase, and to be accurate, the amount of a substance that is used to define standard states is activity, rather than concentration (discussed below). Similarly, amounts of gases are represented by fugacities instead of partial pressures. The standard state of gases is that of unit fugacity of the pure hypothetical ideal gas at 1 bar and any temperature, that of liquids and solids is unit activity of the pure substance at any temperature or pressure, and that of aqueous species is unit activity in a hypothetical 1 molal solution referenced to infinite dilution at any temperature and pressure. This last one is a bit peculiar owing to its impossibility, but it is necessary since the concentration, and thus the distances between dissolved chemical species, can vary by many orders of magnitude in natural systems on and near Earth's surface. Furthermore, since aqueous species are dissolved in a medium that has its own thermodynamic properties, such as water, the interactions between the solvent and dissolved species must also be accounted for in any standard state of aggregation (see Box 19.2).

Box 19.2 G^0 as a function of temperature and pressure and the equilibrium constant.

Many texts incorrectly state that the definition of standard state for all phases specifies a pressure of 1 bar (e.g. 65). However, a cursory glance at the equation that describes how values of the standard-state Gibbs energy of a system or substance at any temperature and pressure, $G^0_{P,T}$, differ from that at the *reference* temperature of 25°C and pressure of 1 bar, $G^0_{P_r,T_r}$, quickly shows why this is wrong for all phases other than gases:

$$G^0_{P,T} - G^0_{P_r,T_r} = -S^0_{P_r,T_r}(T - T_r) + \int_{T_r}^{T} C^0_{P_r} dT - T\int_{T_r}^{T} C^0_{P_r} d\ln T + \int_{P_r}^{P} V^0 dP, \qquad (19.e)$$

where $S^0_{P_r,T_r}$ refers to the standard molal entropy of the species at the reference pressure and temperature, $C^0_{P_r}$ stands for the isobaric molal heat capacity at the reference pressure, and V^0 designates the standard molal volume. The fourth term on the right-hand side shows how standard-state Gibbs energy changes as a function of pressure when temperature is held

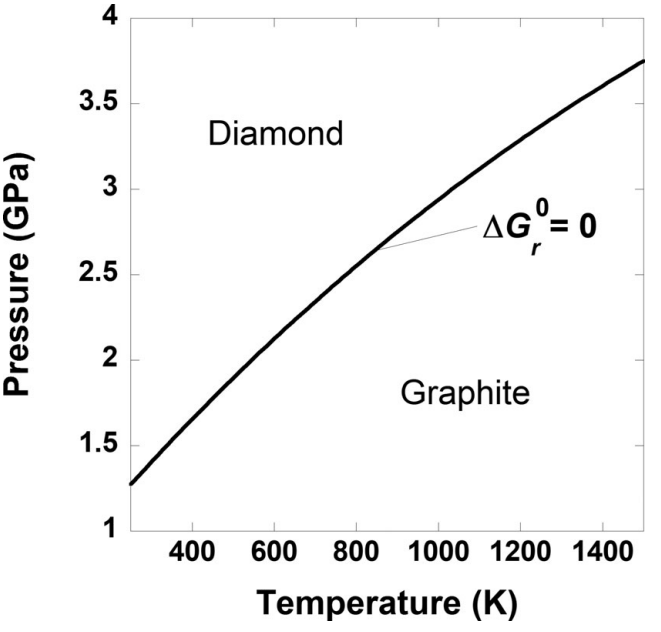

Box Figure 1 A phase diagram for carbon. The curve represents the set of temperatures and pressures where graphite and diamond are in equilibrium, $\Delta G_r^0 = 0$.

constant, $\left(\frac{\partial G^0}{\partial P}\right)_T$. Adding the provision that 1 bar is part of the standard state for solids, liquids, and aqueous species would neglect the volume integral in (19.e) and thus its contribution to the standard-state Gibbs energy. The equilibrium between graphite and diamond further illustrates this point.

The simplified carbon phase diagram presented in Box Figure 1 shows the combinations of temperature and pressure at which graphite and diamond are in equilibrium; that is, $\Delta G_r^0 = 0$ for

$$C_{\text{graphite}} \rightleftharpoons C_{\text{diamond}}. \qquad (19.f)$$

That is, the *standard-state* Gibbs energies of graphite and diamond are equal on this line. Another way to look at this is to use the more intuitive, and aptly named, equilibrium constant, K. The value of K for (19.f) is 1 for the temperatures and pressures that define the curve in Box Figure 1. Values of K are related to the standard-state Gibbs energy via:

$$K = e^{-\left(\frac{\Delta G_r^0}{RT}\right)}. \qquad (19.g)$$

Again, if a pressure of 1 bar were set for the standard-state values of ΔG_f^0 for graphite and diamond, it would be impossible to account for the impact of pressure on the equilibrium state between graphite and diamond. In fact, there would be no stability field for diamond without elevated pressure, no matter the temperature.

For the interested reader, the first three terms on the right-hand side of (19.e) result from taking into account that both enthalpy and entropy are integrals of C_P^0 and thus represent how these thermodynamic functions vary with temperature at constant pressure:

$$C_P^0 = \left(\frac{\partial H^0}{\partial T}\right)_P = T\left(\frac{\partial S^0}{\partial T}\right)_P. \qquad (19.h)$$

If one knows how C_P^0 varies with temperature, then $G_{P,T}^0$ can be calculated for temperatures and pressures other than 25°C and 1 bar. This is rather straightforward for many liquids, gases, and solids; the widely used Maier–Kelley formulation for $C_P^0(T)$ is used: $C_P^0(T) = a + bT + cT^{-2}$. Regression of experimental calorimetry data and/or estimation schemes can be used to determine species-specific values of a, b, and c. However, in the aqueous state, expressions for C_P^0 and V^0 as a function of temperature – and pressure – are more complex due to the interactions of aqueous species with the solvent. The revised Helgeson–Kirkham–Flowers (HKF) equations of state are commonly used to calculate the standard-state thermodynamics properties of aqueous species at temperatures and pressures other than 25°C and 1 bar (see 79–85). The requisite thermodynamic data and equation-of-state parameters for using this model for thousands of aqueous species have been published in the literature (see 50 for a summary of organic compounds, 86 for a summary of minerals, and 87 for inorganic aqueous species, among many others). The *SUPCRT92* software package (80) is commonly used to calculate standard-state thermodynamics properties of species as a function of temperature and pressure using the revised HKF model. In the *R* language and computing environment, *CHNOSZ* has many of the capabilities of *SUPCRT92*, as well as a variety of plotting and other functions (88: chnosz.net).

In many biological applications, the so-called biochemical standard state is used, a term that is typically not rigorously defined (see 56, 89, 90). The Interunion Commission on Biothermodynamics (91) *recommends* that the biochemical standard state should correspond to pH = 7, and the temperature should be 25°C or 37°C, the ionic strength should be set by a 0.1 M KCl solution, concentrations can be used in place of activities, and the concentrations of a group of similar species can be added together and treated as one species (i.e. $[ATP] = [ATP^{4-}] + [HATP^{3-}] + [H_2ATP^{2-}] + [MgATP^{2-}] \ldots$). Although it is relatively straightforward to convert thermodynamic data reported in the biochemical standard state to the traditional chemical standard state for pH and ionic strength, using it is complicated by the fact that the exact version of the biochemical standard state being used is often not specified (i.e. which of the *recommendations* noted above are being followed). For instance, one of the most widely cited papers on the thermodynamics of chemical reactions in the biochemical literature (92) defines a biological standard state similar to one by the Interunion Commission on Biothermodynamics, but also reports so-called observed Gibbs energies that, in addition to fulfilling the biochemical standard state, also sets the ionic strength to 0.25 and a free Mg^{2+} concentration to 0.001 M. Another problem with the biochemical standard state is that some of the researchers who use it and

want to expand it report values of standard Gibbs energies of formation from the elements, ΔG_f^0, for some species to be zero simply because they do not have thermodynamic data for them (see 90). Clearly, this violates the basis of Gibbs energies and enthalpies being based on the Gibbs energy of formation from the elements, which are 0 in their respective reference states at 25°C and 1 bar. This introduces enormous errors that cannot be corrected like pH and ionic strength can be. In addition, many of those who use the biological standard state to compute Gibbs energies of processes rarely use the reaction quotient term, Q, which takes into account composition of the solution, the impact of which is seen in the example calculations presented below. Furthermore, it is worth pointing out that pH 7 only defines solution neutrality ($a_{H^+} = a_{OH^-}$) at 25°C and 1 bar in pure water. Neutral pH at 37°C is 6.81, and at 150°C and 5 bars it is 5.82 ($pH = -\log a_{H^+}$). Finally, if the preceding paragraphs have failed to demystify what standard states are, simply remember that they are about purity (composition) and the elements, and that they are only part of calculating the Gibbs energy of a reaction.

The Gibbs energy of a chemical reaction, ΔG_r, is a function of temperature, pressure, and the composition of the system – not just the activities of the reactants and products of the reaction of interest, but also the concentrations of all of the other chemical species in the system:

$$\Delta G_r = \Delta G_r^0 + RT \ln Q_r, \tag{19.3}$$

where R represents the gas constant and T denotes temperature in Kelvin (see Figure 19.1). The standard-state Gibbs energy of reaction, ΔG_r^0, is simply equal to the difference in the standard-state Gibbs energies of the products and reactants in a reaction, both multiplied by their respective stoichiometric coefficients, v_i:

$$\Delta G_r^0 = \sum_i v_i \Delta G^0_{\text{products}} - \sum_i v_i \Delta G^0_{\text{reactants}}, \tag{19.4}$$

as shown in (19.2) above for reaction (19.1). The reaction quotient, Q_r, a frequently neglected term, is essential to quantifying the Gibbs energy of any reaction that an organism is catalyzing to gain energy. It is responsible for bringing compositional reality into the accurate computation of ΔG_r and is calculated as the product of the activities of the reactants and products, a_i, in a chemical reaction raised to their stoichiometric coefficients, v_i:

$$Q_r = \prod_i a_i^{v_i}. \tag{19.5}$$

Evaluating (19.3)–(19.5) requires that a mass- and charge-balanced reaction has been written to represent a process, and therefore that the identities of all of the product species are known. In some cases, this becomes difficult to ascertain since many common biological elements, such as C, N, and S, have many oxidation states and therefore many different ways to balance the transformation of these elements.

As an example, Q_r for the sulfate reduction shown in Box 19.1, reaction (19.b) is

$$Q_r = \frac{a_{HS^-} a_{H_2O}}{a_{SO_4^{2-}} a_{H_2}^4 a_{H^+}}. \tag{19.6}$$

If only standard-state values of Gibbs energies were used to calculate ΔG_r for (19.b), the resulting calculation would only be valid for activities of all of the species in this reaction being 1 (see Section 19.4 for examples). Since these activities are set by the standard state, it would be equivalent to having 1 molal concentrations of each species in an infinitely dilute solution – an impossible situation. Imagine an environment in which the concentration of all five of these species is 1 molal. At 25°C and 1 bar, this would be a pH of 0 and far beyond the solubility of H_2. Ignoring the Q term when calculating the Gibbs energies of chemical reactions is effectively ignoring physical reality. Using only standard electrical potentials (E^0) to calculate the energetics of reactions is similarly untethered from physical possibilities (see 93).

The way that nonideal conditions (i.e. nonstandard states) are quantified is to use activities in place of concentrations and fugacities instead of partial pressures of gases when evaluating the Q_r term. The concepts of fugacity and activity were developed to account for thermodynamic deviations between ideal and observed behavior (see 94). By close analogy, the ideal gas law only describes the relationship between the amount, temperature, pressure, and volume of a gas ($nRT = PV$) within certain limits of these parameters. When a gas is very concentrated, this simplistic law breaks down and requires additional terms to describe the relationships among the variables in it. Similarly, activity and fugacity account for the nonideal behavior of substances when they are under relatively high concentrations and/or exposed to temperatures and pressures that are far beyond their reference temperatures and pressures. They can be thought of as the effective thermodynamic concentrations of liquids, solids, gases, and aqueous species.

Values of activity are calculated from the concentration of a substance, C, and its activity coefficient, γ: $a = C\gamma$ (a more accurate representation of this relationship is $a = \gamma(C/C^0)$, where C^0 stands for a substance's concentration in the standard state – activity and activity coefficients do not have units). There is a vast and complex literature on how to measure and compute values of γ (e.g. see 66, 83, 85, 95), but suffice to say that they are typically calculated rather than measured for a particular set of conditions. A commonly used model to calculate activities for aqueous species that incorporates elevated temperatures, pressures, and ionic strengths is the extended version of the Debye–Hückel equation (96). Software such as *Geochemist's Workbench* (www.gwb.com) and *PHREEQC* (www.usgs.gov/software/phreeqc) is commonly used to compute activities, as well as to carry out speciation calculations.

Related to the concept of activity is that of speciation. In solution, a given chemical species, especially charged ones, is partitioned among a variety of forms. For instance, in seawater, total sulfate concentration is about 28 mM, and though sulfate exists primarily as SO_4^{2-} at 18.1 mM, the remainder of it is complexed with cations commonly found in seawater. Abundant complexes include $NaSO_4^-$ (7.6 mM), $MgSO_4^0$ (6.2 mM), $CaSO_4^0$

(0.8 mM), and KSO_4^- (0.2 mm). Any calculation of Q_r should take such speciation into account, as well as the activity coefficient of SO_4^{2-}, which in seawater at 25°C and 1 bar is 0.16. Thus, the activity of SO_4^{2-} in seawater at 25°C and 1 bar is 0.0029, nearly an order of magnitude lower than its total concentration of 0.028 M.

Analogous to activity, fugacity (f) is the thermodynamic equivalent of pressure, taking into account the differences between the mechanical pressure exerted by a gas (P) and its effective pressure: $f = P\chi$, where f takes on units of pressure such as bars and the fugacity coefficient, χ, is unitless (see 97).

19.4 Temperature, Pressure, and Composition Affecting *G*

The amount by which variable temperature, pressure, and composition affect the Gibbs energies of chemical reactions can vary tremendously (see 89). Although a number of studies have appeared in the literature demonstrating how different combinations of these variables impact reaction energetics (discussed below), the impact that each of these variables can have alone, and in various combinations, is demonstrated here by using the low-energy metabolism known as hydrogenotrophic acetogenesis:

$$2CO_{2(aq)} + 4H_{2(aq)} \rightarrow CH_3COO^- + H^+ + 2H_2O. \quad (19.7)$$

The curves in Figure 19.3a show the values of $\Delta G^0_{19.7}$ from 0°C to 150°C and the values of ΔG_r for the same reaction under different compositional conditions that characterize high- and low-energy states (the activities of CO_2, H_2, and CH_3COO^- and pH are taken to be 10^{-3}, 10^{-8}, and 10^{-4} and 5 for the low-energy case and $10^{-1.3}$, 10^{-3}, and $10^{-8.5}$ and 9 for the high-energy scenario, respectively). For reference, the diamond shape in Figure 19.3a shows the Gibbs energy of (19.7) under conditions corresponding to the biological standard state, $\Delta G^{0'}_r$, which is more exergonic than even the high-energy scenario, so perhaps it is not very relevant to natural systems. Although the values of ΔG^0_r, the traditional chemical standard-state Gibbs energy, fall between those of the high- and low-energy scenarios, they are much closer to the high-energy state. Notably, ΔG_r for the low-energy case is endergonic throughout the temperature range considered here. Therefore, if one were to use standard-state values of Gibbs energies to quantify how much energy acetogens are gaining by catalyzing (19.7) – at any temperature – when the chemical composition of the system was that specified for the low-energy case, then the direction of the reaction would be wrong: fermentation of acetate (the reverse of (19.7)) would be predicted rather than acetogenesis. Most natural environments could be described by compositions between the high- and low-energy scenarios described here and therefore have values of ΔG_r between the two lines representing them.

The quantitative impact of different pressures on (19.7) is shown in Figure 19.3b. Here, each curve represents ΔG_r of this reaction for activities of CO_2, H_2, and CH_3COO^- and pH equal to $10^{-1.7}$, 10^{-3}, and 10^{-6} and 7, respectively, at saturation pressure (P_{SAT} – just enough pressure to keep water liquid), 250 bars, and 2500 bars. It is clear that values of

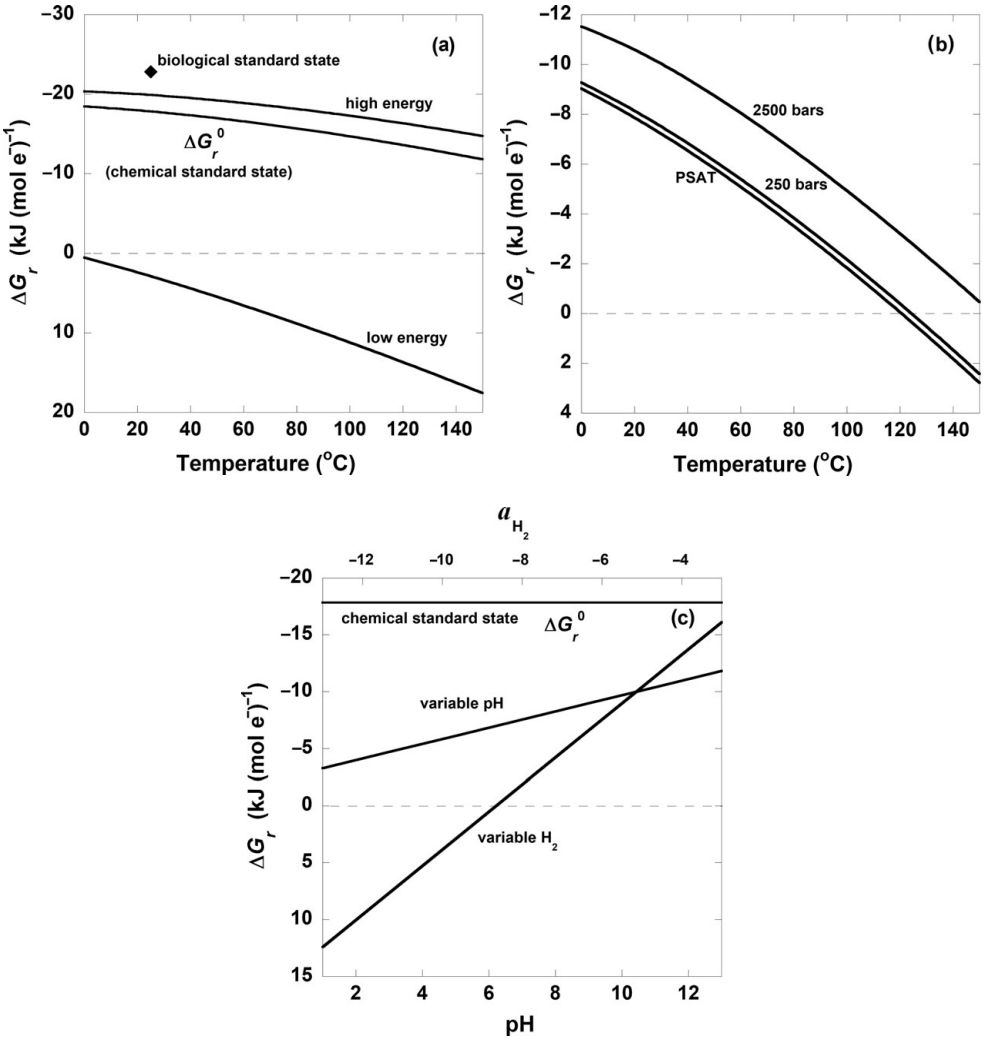

Figure 19.3 Gibbs energies of hydrogenotrophic acetogenesis, $2CO_{2(aq)} + 4H_{2(aq)} \rightarrow CH_3COO^- + H^+ + 2H_2O$, as a function of (a) temperature for the biological and traditional chemical standard states as well as low- and high-energy scenarios, (b) temperature and pressure, and (c) pH and activity of hydrogen, a_{H_2}.

ΔG_r do not differ much between P_{SAT} and 250 bars, and that the difference between P_{SAT} and 2500 bars is just over 2 kJ (mol e$^-$)$^{-1}$. This is a general feature of the quantitative impact of pressure on the Gibbs energies of catabolic reactions. It should be noted that this only takes into account pressure differences on ΔG_r^0 for (19.7) and that pressure can have large effects on the solubility of gases such as CO_2 and H_2, which can lead to higher activities of these compounds at the high pressures often found in the subsurface. These pressure effects on activities would be represented in the Q_r term.

For many microbial processes, the most important variable effecting values of ΔG_r is the Q_r term, or, in other words, the composition of the system. This can clearly be seen in Figure 19.3c, where ΔG_r for (19.7) is shown as a function of pH and H_2 activity, while temperature, pressure, and the activities of the other constituents of (19.7) are held constant (25°C, 1 bar, activities of CO_2 and CH_3COO^- are $10^{-1.7}$ and 10^{-6}; for variable pH, a_{H_2}= 10^{-6} and for variable a_{H_2}, pH = 7). For reference, ΔG_r^0 for this reaction is shown at 25°C and 1 bar and is a flat line at –17 kJ (mol e^-)$^{-1}$. Note that both ranges of a_{H_2} and pH result in much less exergonic values of ΔG_r than would be calculated by using standard-state values. What is apparent from the stoichiometry of (19.7) and Figure 19.3c is that for every order of magnitude change in a_{H_2}, there is a much larger change in ΔG_r than for each integer change in pH. In fact, the acetogenesis pathway represented by (19.7) is no longer thermodynamically favored at pH 7 once a_{H_2} falls below about $10^{-8.5}$. As a sidenote, the steep dependence of ΔG_r on pH shown in Figure 19.3c is typically even more exaggerated in reactions describing the oxidation and reduction of iron, with added variability depending on which iron minerals are involved in the reaction (see 98).

19.5 Surveying Gibbs Energies in Natural Systems

Because microorganisms have evolved the ability to catalyze a wide variety of redox reactions to gain energy under a broad set of physiochemical conditions, there are usually multiple catabolic strategies capable of sustaining a given ecosystem, particularly in subsurface environments that light does not reach. As a result, many of the studies that have quantified the Gibbs energies or chemical affinities (see Box 19.1) of plausible energy-sustaining reactions in subsurface settings have examined a large set of potential catabolic reactions: the thermodynamic potentials of hundreds of chemical reactions have been reported for submarine hydrothermal systems (99–109), shallow-sea hydrothermal systems (110–117), terrestrial hydrothermal systems (118–124), marine sediments (125–132), the terrestrial subsurface (133–135), serpentinizing systems (136), specific-element systems such as arsenic (137), the ocean basement (138–141), and even extraterrestrial settings (142–145). The majority of these studies focus on chemolithotrophic catabolic strategies because concentrations of specific organic compounds are not commonly reported (for exceptions, see 112, 146–148). In fact, the pairs of electron donors and acceptors that are considered are typically those whose concentrations have been measured, which tends not only to narrow the list of metabolisms considered, but also to establish a somewhat consistent set of metabolic redox pairs that are evaluated for their catabolic potential.

The Gibbs energies reported in the studies mentioned above range from endergonic ($\Delta G_r > 0$) to nearly –160 kJ (mol e^-)$^{-1}$. The amount of energy available from a given reaction varies considerably between study sites and even within them. For example, Shock et al. (120) calculated values of ΔG_r for ~300 reactions using temperature, pressure, and compositional data from dozens of hot springs in Yellowstone National Park, USA. Their results showed that the Gibbs energies for nearly 15% of the reactions that they

considered could be exergonic or endergonic, mostly depending on the composition of the individual hot spring fluids. In a similar study, Lu (149) examined the thermodynamic potential of 740 potential catabolic reactions along a two-dimensional transect in sediments next to a shallow-sea hydrothermal vent and found that 559 are exergonic in at least one location.

Although the large number of reactions considered in these and related studies can seem overwhelming, there are a handful of salient points that can be distilled from them beyond the obvious one that many different metabolisms are possible in any given ecosystem. One observation is that the thermodynamic favorability of reactions involving common powerful oxidants such as O_2 and NO_3^- are not necessarily the most exergonic reactions in some environments: the oxidation of Mn^{2+} by O_2, for instance, can easily be endergonic, while the oxidation of CO by NO_2^- (to CO_2 and N_2) can yield more energy than any reaction involving O_2 (149). Composition tends to have a much bigger impact on the energetics of metabolic reactions than either temperature or pressure. The pH of a fluid is responsible for large differences in the values of ΔG_r for the same reaction, especially for those involving iron (120, 127, 135). The wide range of Gibbs energies available from a given electron acceptor shows that the identity of it is not sufficient to predict the order of electron acceptors used by microorganisms (150), a well-known hypothesis in marine science that asserts that organisms in sediments use terminal electron acceptors in the order of their energetic potential (151–153) – an idea that is ultimately based on standard-state Gibbs energies of reaction and restricted to the oxidation of fermentation products. Finally, it is worth pointing out that quantifying the potential energetic landscape in difficult-to-access subsurface environments can be used to predict where novel catabolic reactions could be happening. This is similar to how both the anaerobic oxidation of methane by sulfate and anaerobic ammonium oxidation were predicted based on the thermodynamic calculations demonstrating the Gibbs energies of these reactions (154, 155).

As noted above, Gibbs energy calculations aimed at revealing metabolic potential and involving organic carbon are relatively rare, or are restricted to a small number of compounds such as acetate and other volatile organic acids (e.g. 112, 123, 125, 130, 135, 147, 148). This is certainly an improvement over the common treatment of representing organic carbon as "CH_2O" and thus having a fixed energetic potential that is typically tied to the Gibbs energy of glucose. This is a convenient way of not dealing with the complexity of naturally occurring organic matter – a vast mixture of compounds that vary in their size, charge, oxidation state, structure, and composition. As an extreme example, it is worth noting that Kevlar (polyparaphenylene terephthalamide) and ethanol are both forms of organic matter, yet their properties are wildly divergent.

Although identifying organic compounds in the subsurface is difficult, characterization techniques are improving (156–159), and the thermodynamic properties of thousands of organic compounds have been reported in the literature (see 50 for a review, and, for more recent studies, see 90, 146, 160). Even if organic compounds cannot be identified, if the average NOSC in them can be, then the standard-state Gibbs energy of oxidation can be estimated (50); the range of ΔG_r^0 for the half-oxidation reactions for organic compounds

varies by at least 23 kJ (mol e^-)$^{-1}$ (50). The reactivity of organic carbon in the subsurface would certainly be better understood if the thermodynamic properties of more organic compounds were known.

19.6 Energy Density

Although a thermodynamic calculation can be useful for determining whether a certain reaction is favored to occur under particular environmental conditions, it does not reveal any information about whether the reaction occurs or at what rates, and therefore how many organisms could be supported by it. Ideally, concentration gradients, rate measurements, and/or modeling tools should be used in conjunction with Gibbs energy calculations (e.g. 106, 134, 161–167) to quantify which reactions are driving the biogeochemistry of a system. However, even in the absence of kinetic information, Gibbs energies of reaction can be scaled to units that reveal information about ecosystems that would be otherwise obscured.

Many of the studies noted in Section 19.5 report the Gibbs energies or affinities of potential catabolic reactions in units of kJ mol^{-1} or kJ (mol e^-)$^{-1}$. The latter provides a common basis on which to compare the potential of many redox reactions, though this tends to leave out disproportionation and comproportionation reactions. However, both energy-per-mole units can give a very misleading view of what are the most energy-yielding reactions in an environment. Reactions involving oxygen as the oxidant are especially relevant. For example, ΔG_r for the oxidation of glucose to CO_2 by O_2 is –117 kJ (mol e^-)$^{-1}$ (for $\log a_{O_2} = -4$, $\log a_{CO_2} = -1.7$, $\log a_{glucose} = -4$, and $\log a_{H_2O} = 0$ at 25°C and 1 bar). Keeping the activities of everything else constant and lowering the activity of O_2 by ten orders of magnitude ($\log a_{O_2} = -14$) results in ΔG_r = –103 kJ (mol e^-)$^{-1}$, only a 12% change ($\log a_{O_2}$ would have to be lowered to –86.4 to make this reaction endergonic; for reference, this would be equivalent to about 1000 molecules of O_2 in a volume of water equivalent to the volume of the Milky Way). Even if a concentration of O_2 corresponding to $\log a_{O_2} = -14$ could be measured, any environment characterized with this amount of oxygen would be considered anoxic. Yet, a straightforward thermodynamic calculation shows that it is very exergonic, implying that it should be a likely metabolic activity in the environment. If one presents the results of the same calculations in terms of energy densities (e.g. 103, 127), then about 0.01 kJ (kg H_2O)$^{-1}$ would be available in the high-O_2 case and 10^{-12} J (kg H_2O)$^{-1}$ in the latter, if all of the O_2 could be used instantaneously (typically, energy densities are calculated by multiplying the concentration of the limiting reactant in a reaction by its Gibbs energy, taking into account the stoichiometry of the reactants).

On the low end of the energy spectrum, ΔG_r of glucose oxidation by sulfate, for example, is –21 kJ (mol e^-)$^{-1}$ (for $\log a_{HS^-} = -5$, pH = 8, $\log a_{CO_2} = -1.7$, $\log a_{glucose} = -4$, $\log a_{H_2O} = 0$, and $\log a_{SO_4^{2-}} = -1.7$ at 25°C and 1 bar), which is about one-fifth of ΔG_r for the analogous reaction with O_2 as the oxidant – when the activity of O_2

is 10^{-14}. The energy density of the sulfate reaction is nearly 0.6 kJ (kg H_2O)$^{-1}$, more than even the high-O_2 activity calculations. Interpreting these results is not straightforward: on a molar or per-electron basis, O_2 yields far more energy than sulfate, no matter what the activity of O_2 is, but the energy density of sulfate plus glucose is greater than that of the analogous high-O_2 scenario. One would not expect sulfate reduction to be a prominent glucose oxidation pathway when oxygen is abundant, but it certainly makes sense that sulfate reduction is a more dominant glucose oxidation pathway when oxygen concentrations are below what is currently measurable. Clearly, some combination of common sense and other data will be useful for interpreting the meaning of thermodynamic calculations of catabolic potential, regardless of what units are used.

The units that have been reported for the Gibbs energy calculations summarized above tend to correlate with the environmental system being examined. For example, values of ΔG_r in deep-sea hydrothermal systems tend to be reported in units of J (kg H_2O)$^{-1}$ because these calculations are based on the *in silico* mixing of different masses of fluids that drastically differ in temperature and composition. With different ratios of hydrothermal fluid to seawater and highly variable concentrations of electron donors and acceptors in hydrothermal fluid, the Gibbs energies available for a given reaction from mixing fluids can vary by many orders of magnitude in these units. Typically, the most exergonic reactions for a particular ratio of hydrothermal fluid to seawater are the ones that are reported in these studies: H_2S, CH_4, H_2, and Fe^{2+} oxidation can provide more than 1000 J/kg H_2O (99), and H_2 oxidation can provide up to 3700 J /kg H_2O when hydrothermal fluids from ultramafic systems mix with seawater (100). However, under unfavorable mixing ratios, the amount of energy available from some potential catabolic reactions, such as Fe^{2+} and H_2S oxidation, can be four to eight orders of magnitude lower than the most optimal conditions (104).

The practice of reporting both molal Gibbs energies of potential catabolic reactions and energy densities for some systems (e.g. shallow-sea hydrothermal, marine sediment, and terrestrial systems) is growing (e.g. 110, 126, 127, 133, 149). These studies all show very different results when Gibbs energies are reported in both molal and density units. For instance, LaRowe and Amend (127) compared the Gibbs energies of 18 reactions in three marine sedimentary environments characterized by different physiochemical conditions, varying mostly in composition. They showed that when values of ΔG_r were normalized by the concentration of the limiting reactant (i.e. Gibbs energies were presented as energy densities), the order of the most energy-rich reactions changed considerably and the energy available from different reactions varied by about six orders of magnitude per cm^3 of sediment. Furthermore, they showed that trends in cell abundance as a function of depth do not follow the most exergonic reaction – per mole of substrate – but by those with the highest energy densities.

A global overview of Gibbs energy densities of chemolithotrophic metabolisms in terrestrial hot springs, shallow-sea hydrothermal systems (<200 m water depth), and deep-sea hydrothermal systems is shown in Figure 19.4. The Gibbs energies of potential catabolic reactions consisting of different combinations of 19 electron acceptors and

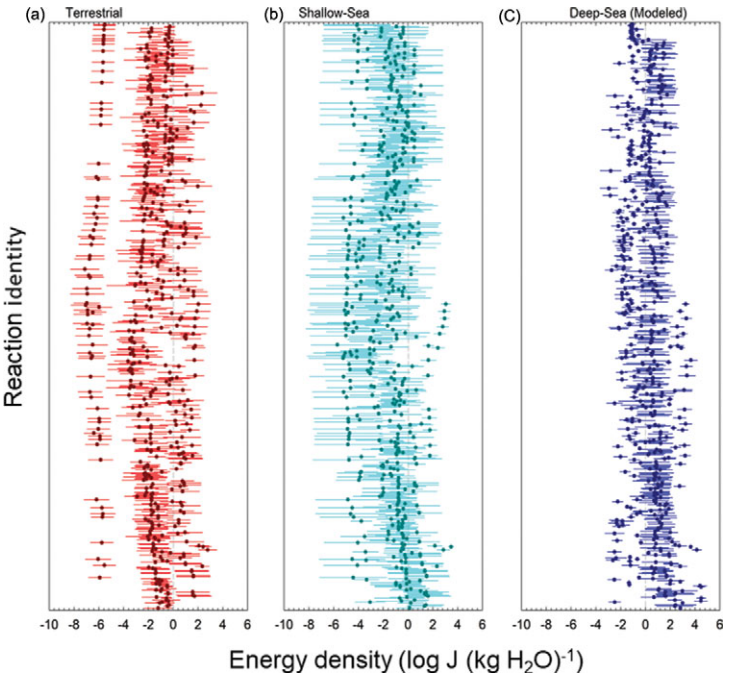

Figure 19.4 Global overview of Gibbs energy densities of chemolithotrophic metabolisms in (a) terrestrial hot springs, (b) shallow-sea hydrothermal systems (<200 m water depth), and (c) deep-sea hydrothermal systems. The Gibbs energies of potential catabolic reactions consisting of different combination of 19 electron acceptors and 14 electron donors were evaluated for 326 data sets describing the geochemistry of 30 distinct systems. The horizontal bars represent the ranges of energy densities for a given reaction and the dots refer to the average energy density of that reaction. Of the 740 reactions considered, 571 are exergonic at one or more sites. The reactions are ordered from the most exergonic to the least based on the Gibbs energies per electron transferred (not shown). Because the compositions of deep-sea hydrothermal systems are often reported as those of calculated end-member hydrothermal fluids, which are typically too hot for life, the results shown in (c) were generated by computing the energy densities of this end-member hydrothermal fluid mixed with enough seawater such that the resulting fluid was 72°C. See (149) for details.

Reproduced with permission of Guang-Sin Lu, PhD thesis (2018), University of Southern California, figure 5.4.

14 electron donors were evaluated for 326 data sets describing the geochemistry of 30 distinct systems. Of the 740 reactions considered, 571 are exergonic at one or more sites. The reactions are ordered from the most exergonic to the least based on the Gibbs energies per electron transferred. Because the compositions of deep-sea hydrothermal systems are often reported as those of calculated end-member hydrothermal fluids, which are typically too hot for life, the results shown in Figure 19.4c were generated by computing the energy densities of this end-member hydrothermal fluid mixed with enough seawater such that the resulting fluid was 72°C, equal to the mean temperature for the terrestrial hot springs and shallow-sea hydrothermal systems represented in the other two

panels in Figure 19.4 (see 149 for details). It can be seen that for many of these reactions, the amount of energy available from a particular combination of electron donors and acceptors varies by many orders of magnitude, reflecting the compositional diversity of global hydrothermal systems. Furthermore, these energy densities span nearly 12 orders of magnitude. The reactions in deep-sea systems tend to have higher energy densities and the reactions in shallow-sea systems tend to show broader ranges. Although there is a sigmoidal pattern for ordering the Gibbs energies of these reactions per electron transferred (see 149), there is no such pattern here. This is because when Gibbs energies are presented in energy density units, directly accounting for the concentration of the limiting electron donor or acceptor, the order of which reaction is most energy yielding can change dramatically.

19.7 Time

Time plays a number of roles in determining the energy limits for life. On a fundamental level, active organisms must be able to catalyze redox reactions faster than they are catalyzed abiotically if they are to gain energy from them. This observation has been more colorfully expressed as "things that burst into flame are not good to eat" (168). Iron oxidation is one such potential metabolism. Although the oxidation of Fe^{2+} with O_2 is a very exergonic reaction under most environmental conditions, the abiotic rate of this process is so fast under certain combinations of pH and temperature that organisms cannot take advantage of the disequilibria. This has been shown to be the case in samples taken from lakes and springs in Switzerland (no biological catalysis for pH $>$7.4) and hot springs in Yellowstone National Park (no biological catalysis for pH $>$ 4.0, at elevated temperatures) (169). Similarly, sulfide oxidation can proceed so quickly in hyperthermophilic settings that isolates capable of catalyzing this reaction, such as *Thermocrinis ruber*, cannot gain energy from it (170).

Microorganisms that are not competing with the abiotic catalysis of potential catabolic reactions still must use energy to combat the slow, abiotic decay of biomolecules such as the depurination of nucleic acids and the racemization of amino acids (18, 20), reactions that accelerate as temperature increases (64, 171). These most basic functions are part of what is known as basal maintenance functions, the absolute minimum flux of energy required to keep a cell viable. Because the rates of biomolecular repair likely approach that at which they are needed, it is difficult to determine the lowest amount of power on which a microorganism can survive. However, marine sediments, with their potential to record environmental data over geologic timescales, can serve as natural laboratories to constrain the basal power limits for life. Geochemical data, cell counts, and modeling efforts have been combined to estimate that microorganisms living in sediments under the South Pacific Gyre are metabolizing organic carbon with oxygen mostly at 50–3350 zW (41). In the same study, the authors hypothesize that an organism could survive on as little at 1 zW.

It is worth clarifying that the lower power limits for life should not be confused with mechanistic arguments that have been made regarding microbial activity and energy minima (see 172). Essentially, it has been proposed that microorganisms require a minimum amount of Gibbs energy from a catabolic reaction (75, 173–175) that is significantly less than $\Delta G_r < 0$. Models that make use of this essentially stipulate that once the Gibbs energy of a particular catabolic reaction dips beneath a given minimum, microorganisms can no longer catalyze the reaction to gain energy (see 78 for an overview). A lower microbial power limit, on the other hand, is simply a flux of energy large enough to keep the cell viable.

19.8 The Cost of Anabolism

As noted above, it is difficult to decipher how microorganisms partition the energy that they get from the environment. However, no matter what state microorganisms are in – growing, maintaining, or some low-level form of dormancy – they must make and/or repair biomolecules to exist for extended periods of time. The identities and quantities of these biomolecules are not well known, nor is the rate at which they must be replaced. What we can determine is the amount of energy associated with the reactions that describe biomolecule synthesis under the temperature, pressure, and compositional conditions prevailing in the deep biosphere. Efforts to do this fall into two groups: (1) those that have sought to determine whether particular organic compounds and biomolecules are thermodynamically favored to be abiotically synthesized under, typically, hydrothermal conditions; and (2) those that quantify the amount of energy required to build the biomolecules that constitute a cell under a variety of environmental conditions (for a review, see 176). Falling into the first group, calculations have shown that the abiotic formation of alkanes, alkenes, alcohols, ketones, aldehydes, carboxylic acids, amino acids, nucleic acid bases, and monosaccharides can be favored to form when particular hydrothermal fluids mix with seawater and kinetic barriers are assumed to prevent carbon transformations to CO_2 or CH_4 (177–181).

The second group of studies focused on the energetics of organic synthesis and quantified the amount of energy that is required to build most of the biomolecules that constitute a cell in the proportions that exist in a model microorganism, *Escherichia coli* (182). McCollom and Amend (48) calculated the Gibbs energy required to make all of the biomonomers that make a cell, starting from inorganic precursor molecules (HCO_3^- (NH_4^+ and NO_3^-), HPO_4^{2-} (H_2S and SO_4^{2-})) under microoxic and anoxic oxidation states. The cost of making biomonomers was 13–15 times higher in the microoxic environment than the anoxic one, depending on the sources of N and S. In an extension of this study, LaRowe and Amend (49) assessed the amount of energy associated with making the same set of biomolecules, but also quantified the role of pressure and used a wider range of redox conditions, temperatures, sources of C, N, and S, and cell sizes. Taken together, environmental variables – and the range of cell sizes – lead to an approximately four orders of magnitude difference between the number of microbial cells that can be made from a Joule

of Gibbs energy under the most (5×10^{11} cells J^{-1}) and least (5×10^{7} cells J^{-1}) ideal conditions.

Finally, a few authors have published calculations in which they have quantified the amount of energy that it takes to synthesize microbial biomass due to the disequilibria resulting from mixing seawater with hydrothermal fluids of variable composition. Amend and McCollom (183) focused on the early Earth, while Amend et al. (99) analyzed how hydrothermal fluids whose compositions were influenced by different water–rock interactions impacted the energetics of biomass synthesis. They showed that the most energetically favorable temperatures were between 22°C and 32°C in general, and that hydrothermal fluids that interacted with peridotite and troctolite–basalt hybrid rock systems created the most favorable energetic conditions for producing biomass, *yielding* up to 900 J per g dry cell mass.

19.9 Concluding Remarks

What combination of natural variables defines the limits to life? The discovery of abundant life in the subsurface has expanded this search to: How deep life can exist? How long can it maintain itself under nearly isolated conditions? And what is the minimum power that it can get by on? One way to address these questions is to determine where and when microorganisms no longer get energy as fast as they need it. In the deep subsurface, this threshold will likely be defined by the power required to repair biomolecules. Essential biomolecules such as nucleotides, amino acids, saccharides, and lipids all undergo abiotic decay through a variety of reactions, including racemization, methylation, deamination, isomerization, radiation exposure, and hydrolysis, while biomacromolecules like DNA, RNA, and proteins can become cross-linked and/or unfolded. The rates of all of these processes depend on the environmental context, particularly temperature. Repairing biomolecules requires energy, and the acquisition of energy requires the maintenance of membrane potentials and the ability to transport nutrients and energy substrates across membranes. Although the energetics and rates of amino acid racemization and DNA depurination have received a fair amount of attention (18), it is not known how all of these degradative processes are influenced by the various combinations of physiochemical and temporal extremes that often define subsurface settings. Identifying the biotic fringe in the subsurface will require quantification of how temperature, pressure, and chemical composition impact the rates of biomolecular decay and how much power is available to rectify this decomposition.

Although we do not always have the information needed to evaluate the amount of catabolic power that is used deep below the surface, we often have the requisite information to quantify the Gibbs energy that is available for microbial energy demands as well as the cost of making biomolecules *in situ*. In this chapter, we have reviewed how temperature, pressure, and composition affect the Gibbs energies of chemical reactions associated with staying alive in the deep biosphere and how to accurately quantify it. We have belabored the

point that the traditional chemical standard state refers to the composition of a system and not temperature and pressure (except for gases), and that the chemical composition of an environment is typically much more significant for calculating the Gibbs energy of a catabolic or anabolic reaction than temperature and pressure. The examples provided illustrate that there is no cheap shortcut to quantifying how much energy is associated with a given chemical reaction under specified physiochemical conditions and that care must be taken to interpret the results of these calculations: Gibbs energies are potentials that can be used to quantify the direction of natural processes and are therefore useful for constraining what life is possible of doing in the subsurface or in any environment.

Acknowledgments

We appreciate the comments provided by anonymous reviewers. This work was supported by the NSF-sponsored Center for Dark Energy Biosphere Investigations (C-DEBI) under grant OCE0939564; the NASA Astrobiology Institute – Life Underground (NAI-LU) grant NNA13AA92A; the USC Zumberge Fund Individual Grant; the NASA-NSF Origins of Life Ideas Lab program under grant NNN13D466T; and the Alfred P. Sloan Foundation through the Deep Carbon Observatory. This is C-DEBI contribution 453 and NAI-LU contribution 134.

Questions for the Classroom

1 Why does the usage of Gibbs energies and other thermodynamic properties require standard states?
2 What are the limitations of the biochemical standard state?
3 What are the factors influencing the amount of energy an organism gains by catalyzing redox reactions?
4 What is the advantage of using chemical affinities rather than overall Gibbs energies of reactions to quantify the tendency of a chemical reaction to proceed?
5 What is the utility of reporting the results of Gibbs energy calculations in density rather than molar units? What are the shortcomings?
6 How does the redox state of an environment influence the amount of energy that is required to make biomass?
7 Why does one need to know the identities and concentrations of products in a catabolic reaction to quantify the amount of energy an organism gains from it?
8 Use the *CHNOSZ* software package (chnosz.net) to calculate how different fugacities (partial pressures) of CO_2 impact the Gibbs energies of acetoclastic and hydrogenotrophic methanogenesis. Hint – see the vignette on chemical affinity on the *CHNOSZ* website.
9 Calculate how different fugacities of H_2 impact the Gibbs energies of hydrogenotrophic methanogenesis.

References

1. Regnier P, Friedlingstein P, Ciais P, Mackenzie FT, Gruber N, Janssens IA, et al. Anthropogenic perturbation of carbon fluxes from land to ocean. *Nat Geosci.* 2013;6:597–607.
2. Mackenzie FT, Lerman A, Andersson AJ. Past and present of sediment and carbon biogeochemical cycling models. *Biogeosciences*. 2004;1:11–32.
3. Whitman WB, Coleman DC, Wiebe WJ. Prokaryotes: the unseen majority. *Proc Natl Acad Sci.* 1998;95(12):6578–6583.
4. Parkes RJ, Cragg B, Roussel E, Webster G, Weightman A, Sass H. A review of prokaryotic populations and processes in sub-seafloor sediments, including biosphere:geosphere interactions. *Mar Geol.* 2014;352:409–425.
5. Kallmeyer J, Pockalny R, Adhikari RR, Smith DC, D'Hondt S. Global distribution of microbial abundance and biomass in subseafloor sediment. *Proc Natl Acad Sci.* 2012;109:16213–16216.
6. Edwards KJ, Becker K, Colwell F. The deep, dark energy biosphere: intraterrestrial life on Earth. *Annu Rev Earth Planet Sci.* 2012;40:551–568.
7. Edwards KJ, Wheat G, Sylvan JB. Under the sea: microbial life in volcanic oceanic crust. *Nat Rev Microbiol.* 2011;9:703–712.
8. Orcutt BN, Sylvan JB, Knab NJ, Edwards KJ. Microbial ecology of the dark ocean above, at, and below the seafloor. *Microbiol Molec Biol Rev.* 2011;75:361–422.
9. McMahon S, Parnell J. Weighing the deep continental biosphere. *FEMS Microbiol Ecol.* 2014;87:113–120.
10. Bar-on Y, Phillips R, Milo R. The biomass distribution on Earth. *Proc Natl Acad Sci.* 2018;115:6506–6511.
11. Chapelle FH, Zelibor Jr. JL, Jay Grimes D, Knobel LL. Bacteria in deep coastal plain sediments of Maryland: a possible source of CO_2 to groundwater. *Water Resources Res.* 1987;23:1625–1632.
12. Pedersen K, Ekendahl S. Distribution and activity of bacteria in deep granitic groundwaters of Southeastern Sweden. *Microb Ecol.* 1990;20:37–52.
13. Stevens TO, McKinley JP. Lithoautotrophic microbial ecosystems in deep basalt aquifers. *Science* 1995;270:450–455.
14. Parkes RJ, Cragg BA, Bale SJ, Getliff JM, Goodman K, Rochelle PA, et al. Deep bacterial biosphere in Pacific Ocean sediments. *Nature.* 1994;371:410–413.
15. Gold T. The deep, hot biosphere. *Proc Natl Acad Sci.* 1992;89(13):6045–6049.
16. Balkwill DL. Numbers, diversity, and morphological charateristics of aerobic, chemoheterotrophic bacteria in deep subsurface sediments from a site in South Carolina. *Geomicrobiol J.* 1989;7:33–52.
17. Hoehler TM, Jørgensen BB. Micorbial life under extreme energy limitation. *Nat Rev Microbiol.* 2013;11:83–94.
18. Lever MA, Rogers KL, Lloyd KG, Overmann J, Schink B, Thauer RK, et al. Life under extreme energy limitation: a synthesis of laboratory- and field-based investigations. *FEMS Microbiol Rev.* 2015;39:688–728.
19. D'Hondt S, Inagaki F, Zarikian CA, Abrams LJ, Dubois N, Engelhardt T, et al. Presence of oxygen and aerobic communities from sea floor to basement in deep-sea sediments. *Nat Geosci.* 2015;8:299–304.
20. Jørgensen BB, Marshall IPG. Slow microbial life in the seabed. *Annu Rev Marine Sci.* 2016;8:311–332.
21. LaRowe DE, Burwicz EB, Arndt S, Dale AW, Amend JP. The temperature and volume of global marine sediments. *Geology.* 2017;45:275–278.

22. Magnabosco C, Lin L-H, Dong H, Bomberg M, Ghiorse W, Stan-Lotter H, et al. The biomass and biodiversity of the continental subsurface. *Nat Geosci*. 2018;11:707–717.
23. Cogley JG. Continental margins and the extent and number of the continents. *Rev Geophys Space Phys.* 1984;22:101–122.
24. Anderson BW, Zoback M, Hickman S, Newmark R. Permeability versus depth in the upper oceanic crust: In situ measurements in DSDP Hole 504B, eastern equatorial Pacific. *J Geophys Res.* 1985;90:3659–3669.
25. Becker K. Measurements of the permeability of the sheeted dikes in Hole 504B, ODP Leg 111. In: Becker K et al. eds. *Proceedings of the Ocean Drilling Program Science Results*. College Station, TX: Ocean Drilling Program, 1989, pp. 317–325.
26. Becker K, Langseth M, Von Herzen RP, Anderson R. Deep crustal geothermal measurements, Hole 504B, Costa Rica Rift. *J Geophys Res.* 1983;88:3447–3457.
27. Hickman SH, Langseth M, Svitek. *In situ* permeability and pore-pressure measurements near the Mid-Atalntic Ridge, Deep Sea Drilling Project Hole 395A. In: Hyndman RD, Salisbury MH, eds. *Initial Reports of the Deep Sea Drilling Project*. Washington, DC: US Goverment Printing Office, 1984, pp. 699–708.
28. Becker K. Measurements of the permeability of the upper oceanic crust at Hole 395A, ODP Leg 109. In: Detrick R, Honnorez J, Bryan WB, Juteau T, eds. *Proceedings of the Ocean Drilling Program Science Results*. College Station, TX: Ocean Drilling Program, 1990, pp. 213–222.
29. Winslow DM, Fisher AT, Becker K. Characterizing borehole fluid flow and formation permeability in the ocean crust using linked analytic models and Markov Chain Monte Carlo analysis. *Geochem Geophys Geosyst*. 2013;14:3857–3874.
30. Alt JC. Alteration of the upper oceanic crust: mineralogy, chemistry, and processes. In: Davis EE, Elderfield H, eds. *Hydrogeology of the Oceanic Lithosphere*. Cambridge: Cambridge University Press, 2004, pp. 456–488.
31. Teagle DAH, Wilson DS. Leg 206 synthesis: initiation of drilling an intact section of upper oceanic crust formed at a superfast spreading rate at Site 1256 in the eastern equatorial Pacific. In: Wilson DS, Teagle DAH, Acton GD, Vanko DA, eds. *Proceedings of the Ocean Drilling Program, Initial Reports*. College Station, TX, USA: Ocean Drilling Program, 2007, pp. 1–15.
32. Fisher AT, Alt JC, Bach W. Hydrogeologic properties, processes and alteration in the igneous ocean crust. In: Stein R, Blackman D, Inagaki F, Larsen H-C, eds. *Earth and Life Processes Discovered from Subseafloor Environment – A Decade of Science Achieved by the Integrated Ocean Drilling Program (IODP)*. Amsterdam/New York: Elsevier, 2014, pp. 507–551.
33. Jakosky B, Shock EL. The biological potential of Mars, the early Earth, and Europa. *J Geophys Res Lett Planets*. 1998;103(E8):19359–19364.
34. Michalski JR, Onstott TC, Mojzsis SJ, Mustard J, Chan QHS, Niles PB, et al. The Martian subsurface as a potential window into the origin of life. *Nat Geosci*. 2018;11:21–26.
35. Vance S, Harnmeijer J, Kimura J, Hussmann H, Demartin B, Brown JM. Hydrothermal systems in small ocean planets. *Astrobiology.* 2007;7:987–1005.
36. Bradley JA, Amend JP, LaRowe DE. Survival of the fewest: microbial dormancy and maintenance in marine sediments through deep time. *Geobiology*. 2019;17:43–59.
37. DePaolo DJ. Sustainable carbon emissions: the geologic perspective. *MRS Energy Sustain*. 2015;2:E9.
38. van Bodegom P. Micorbial maintenance: a critical review of its quantification. *Microb Ecol.* 2007;5:513–523.

39. LaRowe DE, Amend JP. Catabolic rates, population sizes and doubling/replacement times of microorganisms in the natural settings. *Am J Sci.* 2015;315:167–203.
40. Jørgensen BB. Shrinking majority of the deep biosphere. *Proc Natl Acad Sci.* 2012;109:15976–15977.
41. LaRowe DE, Amend JP. Power limits for microbial life. *Front Extr Microbiol*. 2015;6:718.
42. Shock EL, Holland ME. Quantitative habitability. *Astrobiology.* 2007;7:839–851.
43. Morita RY. *Bacteria in Oligotrophic Environments: Starvation–Survival Lifestyle*. New York: Chapman & Hall, 1997.
44. D'Hondt S, Spivack AJ, Pockalny R, Ferdelman TG, Fischer JP, Kallmeyer J, et al. Subseafloor sedimentary life in the South Pacific Gyre. *Proc Natl Acad Sci.* 2009;106:11651–11656.
45. Jørgensen BB, Boetius A. Feast and famine – microbial life in the deep-sea bed. *Nat Rev Microbiol.* 2007;5:770–781.
46. Røy H, Kallmeyer J, Adhikari RR, Pockalny R, Jørgensen BB, D'Hondt S. Aerobic microbial respiration in 86-million-year-old deep-sea red clay. *Science.* 2012;336:922–925.
47. Morono Y, Terada T, Nishizawa M, Ito M, Hillion F, Takahata N, et al. Carbon and nitrogen assimilation in deep subseafloor micorbial cells. *Proc Natl Acad Sci.* 2011;108:18295–18300.
48. McCollom TM, Amend JP. A thermodynamic assessment of energy requirements for biomass synthesis by chemolithoautotrophic micro-organisms in oxic and anoxic environments. *Geobiology.* 2005;3:135–144.
49. LaRowe DE, Amend JP. The energetics of anabolism in natural settings. *ISME J.* 2016;10:1285–1295.
50. LaRowe DE, Van Cappellen P. Degradation of natural organic matter: a thermodynamic analysis. *Geochim Cosmochim Acta.* 2011;75:2030–2042.
51. Heijnen JJ, van Dijken JP. In search of a thermodynamic description of biomass yields for the chemotrophic growth of microorganisms. *Biotech Bioeng.* 1992;39:833–858.
52. Russell JB, Cook GM. Energetics of bacterial growth: balance of anabolic and catabolic reactions. *Microbiol Rev.* 1995;59:48–62.
53. Stouthamer AH. A theoretical study on the amount of ATP required for synthesis of micorbial cell material. *Antonie van Leeuwenhoek.* 1973;39:545–565.
54. LaRowe DE, Helgeson HC. Biomolecules in hydrothermal systems: calculation of the standard molal thermodynamic properties of nucleic-acid bases, nucleosides, and nucleotides at elevated temperatures and pressures. *Geochim Cosmochim Acta.* 2006;70:4680–4724.
55. LaRowe DE, Helgeson HC. The energetics of metabolism in hydrothermal systems: calculation of the standard molal thermodynamic properties of magnesium-complexed adenosine nucleotides and NAD and NADP at elevated temperature and pressures. *Thermochim Acta.* 2006;448:82–106.
56. LaRowe DE, Helgeson HC. Quantifying the energetics of metabolic reactions in diverse biogeochemical systems: electron flow and ATP synthesis. *Geobiology.* 2007;5:153–168.
57. Lennon JT, Jones SE. Micorbial seed banks: the ecological and evolutionary implication of dormancy. *Nat Rev Microbiol.* 2011;9:119–130.
58. Nicholson WL, Munakata N, Horneck G, Melosh HJ, Setlow P. Resistence of *Bacillus* endospores to extreme terrestrial and extraterrestrial environments. *Microbiol Mol Biol Rev.* 2000;64:548–572.

59. Kaprelyants AS, Gottschal JC, Kell DB. Dormancy in non-sporulating bacteria. *FEMS Microbiol Rev.* 1993;104:271–286.
60. Stolpovsky K, Fetzer I, Van Cappellen P, Thullner M. Influence of dormancy on microbial competition under intermittent substrate supply: insights from model simulations. *FEMS Microbiol Ecol.* 2016;92:fiw071.
61. Stolpovsky K, Martinez-Lavanchy P, Heipieper HJ, Van Cappellen P, Thullner M. Incorporating dormancy in dynamic microbial community models. *Ecolog Model.* 2011;222:3092–3102.
62. Johnson SS, Hebsgaard MB, Christensen TR, Mastepanov M, Nielsen R, Munch K, et al. Ancient bacteria show evidence of DNA repair. *Proc Natl Acad Sci.* 2007;104:14401–14405.
63. Locey KJ. Synthesizing traditional biogeography with micorbial ecology: the importance of dormancy. *J Biogeogr.* 2010;37:1835–1841.
64. Price PB, Sowers T. Temperature dependence of metabolic rates for microbial growth, maintenance, and survival. *Proc Natl Acad Sci*. 2004;101:4631–4636.
65. Kondepudi D, Prigogine I. *Modern Thermodynamics: From Heat Engines to Dissipative Structures*. New York: John Wiley & Sons, 1998.
66. Anderson GM, Crerar DA. *Thermodynamics in Geochemistry: The Equilibrium Model*. Oxford: Oxford University Press, 1993.
67. Stumm W, Morgan JJ. *Aquatic Chemistry: Chemical Equilibria and Rates in Natural Waters*. 3rd edn. New York: John Wiley & Sons, Inc., 1996.
68. Garrels RM, Christ CL. *Solutions, Minerals, and Equilibria*. New York: Harper & Row, 1965.
69. Prigogine I, Defay R. *Chemical Thermodynamics*. London: Longmans, Green & Co., 1954.
70. de Donder T, Van Rysselberghe P. *Affinity*. Menlo Park, CA: Stanford University Press, 1936.
71. de Donder T. *Lecons de Thermodynamique et de Chimie-Physique*. Paris: Gauthiers-Villars, 1920.
72. van't Hoff JH. *Études de Dynamique Chimique*. Amsterdam: Frederik Muller & Co., 1884.
73. Aagard P, Helgeson HC. Thermodynamic and kinetic constraints on reaction rates among minerals and aqueous solutions. I. Theoretical considerations. *Amer J Sci.* 1982;282:237–285.
74. Jin Q, Bethke CM. Kinetics of electron transfer through the respiratory chain. *Biophys J.* 2002;83:1797–1808.
75. Jin Q, Bethke CM. A new rate law describing microbial respiration. *Appl Environ Microbiol.* 2003;69:2340–2348.
76. Jin Q, Bethke CM. Predicting the rate of microbial respiration in geochemical environments. *Geochim Cosmochim Acta*. 2005;69:1133–1143.
77. Jin Q, Bethke CM. The thermodynamics and kinetics of microbial metabolism. *Am J Sci.* 2007;307:643–677.
78. LaRowe DE, Dale AW, Amend JP, Van Cappellen P. Thermodynamic limitations on microbially catalyzed reaction rates. *Geochim Cosmochim Acta.* 2012;90:96–109.
79. Tanger JC, Helgeson HC. Calculation of the thermodynamic and transport properties of aqueous species at high pressures and temperatures – revised equations of state for the standard partial molal properties of ions and electrolytes. *Am J Sci*. 1988;288:19–98.
80. Johnson JW, Oelkers EH, Helgeson HC. *SUPCRT92* – a software package for calculating the standard molal thermodynamic properties of minerals, gases, aqueous

species, and reactions from 1 bar to 5000 bar and 0°C to 1000°C. *Comput Geosci*. 1992;18:899–947.
81. Shock EL, Oelkers E, Johnson J, Sverjensky D, Helgeson HC. Calculation of the thermodynamic properties of aqueous species at high pressures and temperatures – effective electrostatic radii, dissociation constants and standard partial molal properties to 1000°C and 5 kbar. *J Chem Soc Faraday Trans*. 1992;88:803–826.
82. Helgeson HC, Kirkham DH. Theoretical prediction of thermodynamic behavior of aqueous electrolytes at high pressures and temperatures: 1. Summary of thermodynamic–electrostatic properties of the solvent. *Am J Sci*. 1974;274: 1089–1198.
83. Helgeson HC, Kirkham DH. Theoretical prediction of thermodynamic behavior of aqueous electrolytes at high pressures and temperatures: 2. Debye–Hückel parameters for activity coefficients and relative partial molal properties. *Am J Sci*. 1974;274:1199–1261.
84. Helgeson HC, Kirkham DH. Theoretical prediction of thermodynamic behavior of aqueous electrolytes at high pressures and temperatures: 3. Equation of state for aqueous species at infinite dilution. *Am J Sci*. 1976;276:97–240.
85. Helgeson HC, Kirkham DH, Flowers GC. Theoretical prediction of thermodynamic behavior of aqueous electrolytes at high pressures and temperatures: 4. Calculation of activity coefficients, osmotic coefficients, and apparent molal and standard and relative partial molal properties to 600°C and 5 kb. *Am J Sci*. 1981;281:1249–1516.
86. Helgeson HC, Delany JM, Nesbitt HW, Bird DK. Summary and critique of the thermodynamic properties of rock-forming minerals. *Am J Sci.* 1978;278:1–229.
87. Sverjensky D, Shock EL, Helgeson HC. Prediction of the thermodynamic properties of aqueous metal complexes to 1000°C and 5 kb. *Geochim Cosmochim Acta*. 1997;61:1359–1412.
88. Dick JM. Calculation of the relative metastabilities of proteins using the *CHNOSZ* software package. *Geochem Trans*. 2008;9:10.
89. Amend JP, Shock EL. Energetics of overall metabolic reactions of thermophilic and hyperthermophilic Archaea and Bacteria. *FEMS Microbiol Rev*. 2001;25:175–243.
90. Canovas III PA, Shock EL. Geobiochemistry of metabolism: standard state thermodynamic properties of the citric acid cycle. *Geochim Cosmochim Acta.* 2016;195:293–322.
91. Wadsö I, Gutfreund H, Privalov P, Edsall JT, Jencks WP, Armstrong GT, et al. Recommendations for measurement and presentation of biochemical equilibrium data. *J Biol Chem.* 1976;251:6879–6885.
92. Thauer RK, Jungermann K, Decker K. Energy conservation in chemotrophic anaerobic bacteria. *Bacteriol Rev*. 1977;41:100–180.
93. Amend JP, Teske A. Expanding frontiers in deep subsurface microbiology. *Palaeogeogr Palaeoclimatol Palaeoecol.* 2005;219:131–155.
94. Lewis GN, Randall M. *Thermodynamics and the Free Energy of Chemical Substances*. New York: McGraw Hill, 1923.
95. Pytkowicz RM. *Activity Coefficients in Electrolyte Solutions*. Boca Raton, FL: CRC Press, 1979.
96. Helgeson HC. Thermodynamics of hydrothermal systems at elevated temperatures and pressures. *Am J Sci.* 1969;267:729–804.
97. Appelo CAJ, Parkhurst DL, Post VEA. Equations for calculating hydrogeochemical reactions of minerals and gases such as CO2 at high pressures and temperatures. *Geochim Cosmochim Acta*. 2014;125:49–67.

98. Rowe AR, Yoshimura M, LaRowe DE, Bird LJ, Amend JP, Hashimoto K, et al. *In situ* electrochemical enrichment and isolation of a magnetite-reducing bacterium from a high pH serpentinizing spring. *Environ Microbiol.* 2017;19: 2272–2285.
99. Amend JP, McCollom TM, Hentscher M, Bach W. Catabolic and anabolic energy for chemolithoautotrophs in deep-sea hydrothermal systems hosted in different rock types. *Geochim Cosmochim Acta.* 2011;75:5736–5748.
100. McCollom TM. Geochemical constraints on sources of metabolic energy for chemolithoautotrophy in ultramafic-hosted deep-sea hydrothermal systems. *Astrobiology.* 2007;7:933–950.
101. Shock EL, Holland ME. Geochemical energy sources that support the subseafloor biosphere. The subseafloor biosphere at mid-ocean ridges. In: Wilcock WSD, DeLong EF, Kelley DS, Baross JA, Cary SC, eds. *Geophysical Monograph 144*. Washington, DC: American Geophysical Union, 2004, pp. 153–165.
102. McCollom TM, Shock EL. Geochemical constraints on chemolithoautotrophic metabolism by microorganisms in seafloor hydrothermal systems. *Geochim Cosmochim Acta*. 1997;61:4375–4391.
103. McCollom TM. Geochemical constraints on primary productivity in submarine hydrothermal vent plumes. *Deep-Sea Res Part I Oceanogr Res Pap*. 2000;47:85–101.
104. Houghton JL, Seyfried Jr. WE. An experimental and theoretical approach to determing linkages between geochemical variability and microbial biodiversity in seafloor hydrothermal chimneys. *Geobiology.* 2010;8:457–470.
105. Shock EL, McCollom TM, Schulte MD. Geochemical constraints on chemolithoautotrophic reactions in hydrothermal systems. *Orig Life Evol Biosph*. 1995;25:141–159.
106. LaRowe DE, Dale AW, Aguilera DR, L'Heureux I, Amend JP, Regnier P. Modeling microbial reaction rates in a submarine hydrothermal vent chimney wall. *Geochim Cosmochim Acta.* 2014;124:72–97.
107. Sylvan JB, Wankel SD, LaRowe DE, Charoenpong CN, Huber H, Moyer CL, et al. Evidence for micorbial mediation of subseafloor nitrogen redox processes at Loihi Seamount, Hawaii. *Geochim Cosmochim Acta.* 2017;198:131–150.
108. Reed DC, Breier JA, Jiang H, Anantharaman K, Klausmeier CA, Toner BM, et al. Predicting the response of the deep-ocean microbiome to geochemical perturbation by hydrothermal vents. *ISME J.* 2015;9:1857–1869.
109. Dahle H, Økland I, Thorseth IH, Pedersen RB, Steen IH. Energy landscapes shape micorbial communities in hydrothermal systems on the Arctic Mid-Ocean Ridge. *ISME J.* 2015;9:1593–1606.
110. Price RE, LaRowe DE, Italiano F, Savov I, Pichler T, Amend JP. Subsurface hydrothermal processes and the bioenergetics of chemolithoautotrophy at the shallow-sea vents off Panarea Island (Italy). *Chem Geol*. 2015;407–408:21–45.
111. Amend JP, Rogers KL, Shock EL, Gurrieri S, Inguaggiato S. Energetics of chemolithoautotrophy in the hydrothermal system of Vulcano Island, southern Italy. *Geobiology.* 2003;1:37–58.
112. Rogers KL, Amend JP. Energetics of potential heterotrophic metabolisms in the marine hydrothermal system of Vulcano Island, Italy. *Geochim Cosmochim Acta.* 2006;70:6180–6200.
113. Akerman NH, Price RE, Pichler T, Amend JP. Energy sources for chemolithotrophs in an arsenic- and iron-rich shallow-sea hydrothermal system. *Geobiology.* 2011;9:436–445.

114. Rogers KL, Amend JP, Gurrieri S. Temporal changes in fluid chemistry and energy profiles in the Vulcano island hydrothermal system. *Astrobiology.* 2007;7:905–932.
115. Rogers KL, Amend JP. Archaeal diversity and geochemical energy yields in a geothermal well on Vulcano Island, Italy. *Geobiology.* 2005;3:319–332.
116. Skoog A, Vlahos P, Rogers KL, Amend JP. Concentrations, distributions, and energy yields of dissolved neutral aldoses in a shallow hydrothermal vent system of Vulcano, Italy. *Org Geochem.* 2007;38:1416–1430.
117. Lu G-S, LaRowe DE, Gilhooly III WP, Druschel GK, Fike DA, Amend JP. Chemolithoautotrophic energetics in a shallow-sea hydrothermal system, Milos Island, Greece. *Manuscript in preparation*.
118. Inskeep W, Ackerman GG, Taylor WP, Kozubal M, Korf S, Macur RE. On the energetics of chemolithotrophy in nonequilibrium systems: case studies of geothermal springs in Yellowstone National Park. *Geobiology.* 2005;3:297–317.
119. Inskeep WP, McDermott TR. Geomicrobiology of acid–sulfate–chloride springs in Yellowstone National Park. In: Inskeep WP, McDermott TR, eds. *Geothermal Biology and Geochemistry in Yellowstone National Park*. Bozeman, MT: Montana State University Publications, 2005, pp. 143–162.
120. Shock EL, Holland M, Meyer-Dombard D, Amend JP, Osburn GR, Fischer TP. Quantifying inorganic sources of geochemical energy in hydrothermal ecosystems, Yellowstone National Park, USA. *Geochim Cosmochim Acta.* 2010;74:4005–4043.
121. Spear JR, Walker JJ, McCollom TM, Pace NR. Hydrogen and bioenergetics in the Yellowstone geothermal ecosystem. *Proc Natl Acad Sci.* 2005;102:2555–2560.
122. Vick TJ, Dodsworth JA, Costa KC, Shock EL, Hedlund BP. Microbiology and geochemistry of Little Hot Creek, a hot spring environment in the Long Valley Caldera. *Geobiology.* 2010;8:140–154.
123. Windman T, Zolotova N, Schwandner F, Shock EL. Formate as an energy source for microbial metabolism in chemosynthetic zones of hydrothermal ecosystems. *Astrobiology.* 2007;7:873–890.
124. Costa KC, Navarro JB, Shock EL, Zhang CL, Soukup D, Hedlund BP. Microbiology and geochemistry of great boiling and mud hot springs in the United States Great Basin. *Extremophiles.* 2009;13:447–459.
125. LaRowe DE, Dale AW, Regnier P. A thermodynamic analysis of the anaerobic oxidation of methane in marine sediments. *Geobiology.* 2008;6:436–449.
126. Teske A, Callaghan AV, LaRowe DE. Biosphere frontiers: deep life in the sedimented hydrothermal system of Guaymas Basin. *Front Extr Microbiol*. 2014;5:362.
127. LaRowe DE, Amend JP. Energetic constraints on life in marine deep sediments. In: Kallmeyer J, Wagner K, eds. *Life in Extreme Environments: Microbial Life in the Deep Biosphere*. Berlin: de Gruyter, 2014, pp. 279–302.
128. Wang G, Spivack AJ, D'Hondt S. Gibbs energies of reaction and microbial mutualism in anaerobic deep subseafloor sediments of ODP Site 1226. *Geochim Cosmochim Acta.* 2010;74:3938–3947.
129. Kiel Reese B, Zinke LA, Sobol MS, LaRowe DE, Orcutt BN, Zhang X, et al. Nitrogen cycling of active bacteria within oligotrophic sediment of the Mid-Atlantic Ridge Flank. *Geomicrobiol J*. 2018;35:468–483.
130. Glombitza C, Jaussi M, Røy H. Formate, acetate, and propionate as substrates for sulfate reduction in sub-arctic sediments of Southwest Greenland. *Front Microbiol*. 2015;6:846.
131. Beulig F, Røy H, Glombitza C, Jørgensen BB. Control on rate and pathway of anaerobic organic carbon degradation in the seabed. *Proc Natl Acad Sci*. 2018;155:367–372.

132. Schrum HN, Spivack AJ, Kastner M, D'Hondt S. Sulfate-reducing ammonium oxidation: a thermodynamically feasible metabolic pathway in subseafloor sediment. *Geology.* 2009;37:939–942.
133. Osburn MR, LaRowe DE, Momper L, Amend JP. Chemolithotrophy in the continental deep subsurface: Sanford Underground Research Facility (SURF), USA. *Front Extr Microbiol*. 2014;5:610.
134. Jin Q, Bethke CM. Cellular energy conservation and the rate of microbial sulfate reduction. *Geology.* 2009;37:1027–1030.
135. Kirk MF, Jin Q, Haller BR. Broad-scale evidence that pH influences the balance between microbial iron and sulfate reduction. *Groundwater.* 2015;54:406–413.
136. Canovas III PA, Hoehler TM, Shock EL. Geochemical bioenergetics during low-temperature serpentinization: an example from the Samail ophiolite, Sultanate of Oman. *J Geophys Res Biogeosci.* 2017;122:1821–1847.
137. Amend JP, Saltikov C, Lu G-S, Hernandez J. Micorbial arsenic metabolism and reaction energetics. *Rev Mineral Geochem.* 2014;79:391–433.
138. Edwards KJ, Bach W, McCollom TM. Geomicrobiology in oceanography: microbe–mineral interactions at and below the seafloor. *Trends Microbiol.* 2005;13:449–456.
139. Bach W, Edwards KJ. Iron and sulfide oxidation within the basaltic ocean crust: implications for chemolithoautotrophic microbial biomass production. *Geochim Cosmochim Acta.* 2003;67:3871–3887.
140. Cowen JP. The microbial biosphere of sediment-buried oceanic basement. *Res Microbiol.* 2004;155:497–506.
141. Boettger J, Lin H-T, Cowen JP, Hentscher M, Amend JP. Energy yields from chemolithotrophic metabolisms in igneous basement of the Juan de Fuca ridge flank system. 2013;337–338:11–19.
142. Shock EL. High-temperature life without photosynthesis as a model for Mars. *J Geophys Res Planets*. 1997;102:23687–23694.
143. Zolotov MY, Shock EL. Energy for biologic sulfate reduction in a hydrothermally formed ocean on Europa. *J Geophys Res Planets*. 2003;108:5022.
144. Waite JH, Glein CR, Perryman RS, Teolis BD, Magee BA, Miller G, et al. Cassini finds molecular hydrogen in the Enceladus plume: evidence for hydrothermal processes. *Science*. 2017;356:155–159.
145. Marlow J, LaRowe DE, Ehlman BL, Amend JP, Orphan V. The potential for biologically catalyzed anaerobic methane oxidation on ancient mars. *Astrobiology.* 2014;14:292–307.
146. LaRowe DE, Amend JP. The energetics of fermentation in natural settings. *Geomicrobiology*. 2019;36:492–505.
147. Lever MA. Acetogenesis in the energy-starved deep biosphere – a paradox? *Frontiers in Microbiology*. 2012;2:284.
148. Lever MA, Heuer VB, Morono Y, Masui N, Schmidt F, Alperin MJ, et al. Acetogensis in deep subseafloor sediments of the Juan de Fuca Ridge Flank: a synthesis of geochemical, thermodynamic, and gene-based evidence. *Geomicrobiol J.* 2010;27:183–211.
149. Lu G-S. Geomicrobiology in the Shallow-Sea Hydrothermal System at Milos Island, Greece. PhD thesis. Los Angeles, CA: University of Southern California, 2018.
150. Bethke CM, Sanford RA, Kirk MF, Jin Q, Flynn TM. The thermodynamic ladder in geomicrobiology. *Am J Sci.* 2011;311:183–210.
151. Claypool GE, Kaplan IR. The origin and distribution of methane in marine sediments. In: Kaplan IR, ed. *Natural Gases in Marine Sediments*. New York: Plenum Press, 1974, pp. 99–139.

152. Froelich PN, Klinkhammer GP, Bender ML, Luedtke NA, Heath GR, Cullen D, et al. Early oxidation of organic matter in pelagic sediments of the eastern equatorial Atlantic: suboxic diagenesis. *Geochim Cosmochim Acta.* 1979;43:1075–1090.
153. Stumm W, Morgan JJ. *Aquatic Chemistry: Chemical Equilibria and Rates in Natural Waters*. 3rd edn. New York: John Wiley & Sons, 1996.
154. Reeburgh WS. Methane consumption in Cariaco Trench waters and sediments. *Earth Planet Sci Lett.* 1976;28:337–344.
155. Broda E. Two kinds of lithotrophs missing in nature. *Z Allg Mikrobiol.* 1977;17:491–493.
156. LaRowe DE, Koch BP, Robador A, Witt M, Ksionzek K, Amend JP. Identification of organic compounds in ocean basement fluids. *Org Geochem.* 2017;113:124–127.
157. Hertkorn N, Harir M, Koch BP, Michalke B, Schmitt-Kopplin P. High-field NMR spectroscopy and FTICR mass spectrometry: poweerful discovery tools for the molecular level characterization of marine dissolved organic matter. *Biogeosciences.* 2013;10:1583–1624.
158. Ball GI, Aluwihare LI. CuO-oxidized dissolved organic matter (DOM) investigated with comprehensive two dimensional gas chromatography-time of flight-mass spectrometry (GC × GC-TOF-MS). *Org Geochem.* 2014;75:87–98.
159. Shah Walter SR, Jaekel U, Osterholz H, Fisher AT, Huber JA, Pearson A, et al. Microbial decomposition of marine dissolved organic matter in cool oceanic crust. *Nat Geosci.* 2018;11:334–339.
160. LaRowe DE, Dick JM. Calculation of the standard molal thermodynamic properties of crystalline proteins. *Geochim Cosmochim Acta.* 2012;80:70–91.
161. Dale AW, Regnier P, Van Cappellen P. Bioenergetic controls on anaerobic oxidation of methane (AOM) in coastal marine sediments: a theoretical analysis. *Am J Sci.* 2006;306:246–294.
162. Dale AW, Aguilera DR, Regnier P, Fossing H, Knab NJ, Jørgensen BB. Seasonal dynamics of the depth and rate of anaerobic oxidation of methane in Aarhus Bay (Denmark) sediments. *J Mar Res.* 2008;66:127–155.
163. Dale AW, Regnier P, Knab NJ, Jørgensen BB, Van Cappellen P. Anaerobic oxidation of methane (AOM) in marine sediments from the Skagerrak (Denmark): II. Reaction-transport modeling. *Geochim Cosmochim Acta.* 2008;72:2880–2894.
164. Dale AW, Sommer S, Haeckel M, Wallmann K, Linke P, Wegener G, et al. Pathways and regulation of carbon, sulfur and energy trasnfer in marine sediments overlying methane gas hydrates on the Opouawe Bank (New Zealand). *Geochim Cosmochim Acta.* 2010;74:5763–5784.
165. Dale AW, Van Cappellen P, Aguilera DR, Regnier P. Methane efflux from marine sediments in passive and active margins: estimations from bioenergetic reaction-transport simulations. *Earth Planet Sci Lett.* 2008;265:329–344.
166. Algar CK, Vallino JJ. Predicting microbial nitrate reduction pathways in coastal sediments. *Aquatic Microbial Ecol.* 2014;71:223–238.
167. André L, Pauwels H, Dictor M-C, Parmentier M, Azaroual M. Experiments and numerical modelling of microbially-catalysed denitrification reactions. *Chem Geol.* 2011;287:171–181.
168. Shock EL, Boyd ES. Principles of geobiochemistry. *Elements.* 2015;11:395–401.
169. St. Clair B. *Kinetics, Thermodynamics and Habitability of Microbial Iron Redox Cycling*. Phoenix, AZ: Arizona State Univesity, 2017.
170. Härtig C, Lohmayer R, Kolb S, Horn MA, Inskeep WP, Planer-Friedrich B. Chemolithotrophic growth of the aerobic hyperthermophilic bacterium *Thermocrinus*

ruber OC 14/7/2 on monothioarsenate and arsenite. *FEMS Microbiol Ecol*. 2014;90:747–760.
171. Steen AD, Jørgensen BB, Lomstein BA. Abiotic racemization kinetics of amino acids in marine sediments. *PLoS One.* 2013;8:e71648.
172. Harder J. Species-independent maintenance energy and natural population sizes. *FEMS Microbiol Ecol.* 1997;23:39–44.
173. Schink B. Energetics of synthrophic cooperation in methanogenic degradation. *Microbiol Mol Biol Rev*. 1997;61(2):262–280.
174. Curtis GP. Comparison of approaches for simulating reactive solute transport involving organic degradation reactions by multiple terminal electron acceptors. *Comp Geosci.* 2003;29:319–329.
175. Hoehler TM. Biological energy requirements as quantitative boundary conditions for life in the subsurface. *Geobiology.* 2004;2:205–215.
176. Amend JP, LaRowe DE, McCollom TM, Shock EL. The energetics of organic synthesis inside and outside the cell. *Phil Trans Royal Soc B.* 2013;368:1–15.
177. Amend JP, Shock EL. Energetics of amino acid synthesis in hydrothermal ecosystems. *Science*. 1998;281:1659–1662.
178. Amend JP, Shock EL. Thermodynamics of amino acid synthesis in hydrothermal ecosystems on the early Earth. In: Goodfriend G, ed. *Perspectives in Amino Acid and Protein Geochemistry*. New York: Plenum, 2000, pp. 23–40.
179. Shock EL, Schulte MD. Organic synthesis during fluid mixing in hydrothermal systems. *J Geophys Res Planets*. 1998;103:28513–28527.
180. Shock EL, Canovas III PA. The potential for abiotic organic synthesis and biosynthesis at seafloor hydrothermal systems. *Geofluids.* 2010;10:161–192.
181. LaRowe DE, Regnier P. Thermodynamic potential for the abiotic synthesis of adenine, cytosine, guanine, thymine, uracil, ribose and deoxyribose in hydrothermal systems. *Orig Life Evol Biosph.* 2008;38:383–397.
182. Battley EH. An alternative method of calculating the heat of growth of *Escherichia coli* K-12 on succinic acid. *Biotech Bioeng*. 1991;38:480–492.
183. Amend JP, McCollom TM. Energetics of biomolecule synthesis on early Earth. In: Zaikowski L, Friedrich JM, Seidel SR, eds. *Chemical Evolution II: From the Origins of Life to Modern Society*. Washington, DC: American Chemical Society, 2009, pp. 63–94.